

**2-D ELECTRICAL RESISTIVITY IMAGING**  
**AROUND THE COLLAPSED BUILDINGS OF THE HOUSING ESTATE AT**  
**BARNAWA-NARAYI JUNCTION, KADUNA, KADUNA STATE**

**BY**

**AGBO COMFORT B.Sc.(ABU 2008)**

**M.Sc./SCIE/00152/2009-2010**

**BEING A THESIS SUBMITTED TO THE POSTGRADUATE SCHOOL,**  
**AHMADU BELLO UNIVERSITY,**  
**ZARIA, NIGERIA.**

**IN PARTIAL FULFILLMENT FOR THE AWARD OF**  
**MASTERS OF SCIENCE IN APPLIED**  
**GEOPHYSICS**  
**DEPARTMENT OF PHYSICS**  
**FACULTY OF SCIENCE**  
**AHMADU BELLO UNIVERSITY, ZARIA.**

**NOVEMBER, 2014.**

## **DECLARATION**

I declare that this thesis is my own unaided work. It is submitted for the degree of Masters of Science, at the Ahmadu Bello University, Zaria. It has not been submitted before for any other degree or examination at any other university.

**AGBO, Comfort**

-----

Name of student

Signature

Date

## CERTIFICATION

This thesis titled “**2-D ELECTRICAL RESISTIVITY IMAGING AROUND THE COLLAPSED BUILDINGS OF THE HOUSING ESTATE AT BARNAWA-NARAYI JUNCTION, KADUNA, KADUNA STATE**”, by **AGBO, Comfort** meets the regulations governing the award of degree of Masters of Science (M.Sc.) of Ahmadu Bello University, Zaria, and is approved for its contributions to knowledge and literary presentation.

\_\_\_\_\_  
Chairman, Supervisory Committee  
Dr. K.M. LAWAL

\_\_\_\_\_  
Signature

\_\_\_\_\_  
Date

\_\_\_\_\_  
Member, Supervisory Committee  
Prof. B.B.M. DEWU

\_\_\_\_\_  
Signature

\_\_\_\_\_  
Date

\_\_\_\_\_  
Head of Department  
Dr. U. SADIQ

\_\_\_\_\_  
Signature

\_\_\_\_\_  
Date

\_\_\_\_\_  
Dean, Postgraduate School  
Prof. A. A JOSHUA

\_\_\_\_\_  
Signature

\_\_\_\_\_  
Date

## ACKNOWLEDGEMENT

I express my sincere thanks and appreciation to God Almighty for His grace in my time of need.

I acknowledge the generous and intellectual support of my supervisors, Dr. K.M. Lawal and Prof.B.B.M. Dewu. I appreciate your efforts for finding time to go through this work despite your busy schedule.

To my parents, Mr and MrsJ.A.Agbo, for their love and care. Their awesome sacrifices are etched in my memory, and they are evergreen. To my siblings, for their faith and endless prayers. The labour of their knees restored me.

I am also grateful to my best friend and husband Pharm. Nathaniel Okpokwu, for his selflessness and true friendship.The Uphophomons and OnomeOyedokun for your encouragement and support during the period of my studies. I immensely appreciate you.

My sincere appreciation goes to the Head of Department, Dr. U. Sadiq andMr. J. Osumaje of Physics department, the management and staff of Centre for Geodesy and Geodynamics (CGG), Toro, Bauchi State, The Director, Mr. Abu L.O.I and Mr. Mohammed of Nigeria Geological Survey Agency (NGSA), Barnawa, Kaduna State and MrE.E.Nkitnam of MevHydrosearch and Engineering Services Ltd, Kaduna State.

Special thanks go to my colleagues Mike Asuerimen, Francis Uwaechia, HaliruAdamu, Segun , Larry, Yusuf and Mohammed who encouraged me during the course of my studies and during this research. I appreciate you all. God bless you all.

More modestly though, there are many people who have contributed in various ways to my completion of this thesis and inasmuch as I would like to “observe protocol,” the list is almost certainly endless, such is my debt of gratitude.

## ABSTRACT

Resistivity method is frequently used in environmental studies. Electrical resistivity imaging survey has been carried out at the housing estate located at Barnawa-Narayi junction in Kaduna, Kaduna State in order to investigate the subsurface geological structures which include the possible presence of faults, fractures, voids and clay that may pose danger to the structures that have been constructed, depth to bedrock and thickness of weathered basement (aquiferous zone). A modern and state-of-the-art field instrument, the ABEM Automatic LUND Imaging System (Terrameter SAS 1000 and ES 464) employing the Schlumberger array, was used to accomplish this task by obtaining two-dimensional resistivity data sets along seven profiles within the survey area. The acquired data were processed and interpreted using RES2DINV software to produce the two-dimensional image of the study area. The subsurface images showed that the resistivity range lies between 1 to about 1178 $\Omega$ m, indicating variation in soil matrix, grain size distribution and water saturation. The near surface materials from 0 to a depth of about 2.7m constitute the top soil with relatively high resistivity values ranging from 49 $\Omega$ m to 180 $\Omega$ m were obtained. The decrease in resistivity ranging from 4 $\Omega$ m to 98 $\Omega$ m with thickness of about 10.0m below the top soil indicates saturated soil. The fractured/partially weathered zone has resistivity ranging from 49 $\Omega$ m to 533 $\Omega$ m with thickness between 5.0m and 17.2m. Beyond the fractured/partially weathered basement is the fresh basement with resistivity value ranging from 429 $\Omega$ m to 1178 $\Omega$ m with variable depth to it. This depth in profiles 2 and 4 is 17.2m and in profile 6 it is 14.8m. The basement was not reached in profiles 1, 3, and 5. It appears in form of an intrusion in profile 7 at a depth of about 6.9m. The images suggest the presence of building constraints such as fractures/zones of weakness that may constitute problems to the building foundations. However, the images have not suggested the presence of clay formations. The zones of weakness/fractures discovered within the area of study have resistivity values ranging between 49 $\Omega$ m and 109 $\Omega$ m which could also have led to the collapse of the buildings. The subsurface within the area of study is characterized by sharp variations in the basement relief/topography which probably led to the collapse of the buildings.

## TABLE OF CONTENTS

	<b>Page</b>
<b>TITLE PAGE</b>	i
<b>DECLARATION</b>	ii
<b>CERTIFICATION</b>	iii
<b>ACKNOWLEDGEMENT</b>	iv
<b>ABSTRACT</b>	vi
<b>TABLE OF CONTENTS</b>	vii
<b>LIST OF TABLES</b>	xi
<b>LIST OF FIGURES</b>	xii
<b>CHAPTER ONE</b>	
<b>INTRODUCTION</b>	1
1.1 General Overview	1
1.2 Location of the study Area	3
1.3 Aim and Objectives	6
1.4 Justification of the study	6

## **CHAPTER TWO**

### **LITERATURE REVIEW** 7

- 2.1 Previous Geophysical and Geological Investigations in  
the Study Area 7
- 2.2 General Geology of the Study Area 10

## **CHAPTER THREE**

### **METHODOLOGY** 13

- 3.1 Introduction 13
- 3.2 Fieldwork 13
- 3.3 Choice of the Method 15
- 3.4 Field Procedure 15
- 3.5 Typical Resistivity Values of Earth Materials 20
- 3.6 Theory of Direct Current Resistivity Method 24
- 3.7 Principle of Lund Resistivity Imaging and Instrumentation 28
- 3.8 The ABEM Lund Imaging system 29

## **CHAPTER FOUR**

<b>FIELD RESULTS AND INTERPRETATION</b>	<b>33</b>
4.1 Introduction	33
4.2 Data Processing	33
4.3 Interpretation Technique	35
4.4 Geologic Section from Borehole Data	36
4.5 Typical Resistivity Values from Previous works	38
4.6 Field Results	41
4.6.1 Profile 1	43
4.6.2 Profile 2	43
4.6.3 Profile 3	46
4.6.4 Profile 4	46
4.6.5 Profile 5	49
4.6.6 Profile 6	49
4.6.7 Profile 7	52

## **CHAPTER FIVE**

DISCUSSION, CONCLUSIONS AND RECOMMENDATIONS	57
5.1 Discussion	57
5.2 Conclusions	58
5.3 Recommendations	59
References	60

## LIST OF TABLES

Table 3.1 Coordinates of midpoints along the profiles	19
Table 4.1 A Borehole Lithology of “Salient Shopping Mall”, Barnawa, Kaduna	37
Table 4.2 Typical Resistivity values compiled from previous works	38
Table 4.3 Typical Resistivity values of rock materials from previous works	39
Table 4.4 Resistivity values adopted for this work	40

## LIST OF FIGURES

Figure 1.1 Geological Map of some parts of Kaduna town showing Barnawa which is the Study Area	4
Figure 1.2 Google Image of the Study Area (Barnawa)	5
Figure 2.1 Basement Geological Map of Nigeria Showing the Study Area (After Obaje, 2009)	11
Figure 3.1 Google Image of the Study Area Showing profiles 1 to 7	14
Figure 3.2 The steps used to increase the depth of investigation by (a) Wenner and (b) Schlumberger arrays	16
Figure 3.3 Arrangement of data points in the pseudosections for (a) Wenner and (b) Schlumberger arrays	16
Figure 3.4 A Typical Range of Resistivities of Geologic Materials (ABEM Instruction Manual)	22
Figure 3.5 Resistivities of Rocks, Soils and Minerals (Loke, 2004)	23
Figure 3.6 Schlumberger Electrode Array	26

Figure 3.7 ABEM LUND Imaging System together with Terrameter SAS 1000, ES 464 and other Accessories	32
Figure 4.1 The result of 2D inversion of the Schlumberger array data along profile 1	44
Figure 4.2 The result of 2D inversion of the Schlumberger array data along profile 2	45
Figure 4.3 The result of 2D inversion of the Schlumberger array data along profile 3	47
Figure 4.4 The result of 2D inversion of the Schlumberger array data along profile 4	48
Figure 4.5 The result of 2D inversion of the Schlumberger array data along profile 5	50
Figure 4.6 The result of 2D inversion of the Schlumberger array data along profile 6	51
Figure 4.7 The result of 2D inversion of the Schlumberger array data along profile 7	53
Figure 4.8 ERT images for profiles 7,2,6,5 and 4 arranged in the order in which they appear within the area of study	55
Figure 4.9 ERT images for profiles 3 and 1 arranged in the order in which they appear within the area of study	

## CHAPTER ONE

### INTRODUCTION

#### 1.1 General Overview

Subsurface investigations employing geophysical techniques are of paramount importance in assessing the suitability of an area for the construction of buildings, roads, bridges, etc. It is common knowledge that these structures among other reasons, collapse because appropriate geophysical investigations were not carried out to determine the nature of the subsurface structures. Most of these buildings were built on soils that have inadequate bearing capacity to support the weight of the building. The geology of an area is critical in assessing its suitability for the type of building to be erected. The necessity for site characterization for construction purposes has therefore become very vital so as to prevent loss of valuable lives and properties that always accompany such collapse. Some general reasons why buildings may be susceptible to collapse have been advanced, which include poor quality of building materials, salinity, and old age of buildings(Oyedele,2011). Less frequently mentioned reasons are the subsurface conditions of the ground on which the buildings are sited. Subsurface geological features such as fractures, voids, small depth to bedrock, near – surface depth to water table are among the common constraints to building constructions, especially to their foundations (Ugwu and Ezema, 2013). The cause of rampant failure of building foundations due to subsurface movements giving rise to cracks or structural differential settlement is of great concern to geoscientists and engineers. There is need to distinguish between a continuing movement, which is often more likely to be a problem, and single eventual movement, which may not require repair depending on the extent of damage. In building construction, poor soil stability is one of the factors that cause havoc. This is because some soils are very sensitive to moisture gain or loss. Certain clay soils for instance, can expand multiple times in volume if they get saturated with

water and when there is loss of water in them, they shrink in volume. This expansion and contraction of clayey soils cause foundation cracks on buildings shortly after they are built in the process of their settlement (Egwuonwu et al., 2011). Some settlements are due to unstable soil and structures above concealed cavities or organic materials, while others are due to expansive soils. Sometimes foundation cracks occur because the foundations are located on areas likely to be affected by landslides thereby moving laterally and vertically, usually at different speeds. Settlements could also be due to shock, vibration or regional subsidence (Tomlinsong and Boorman, 1999; Sands, 2002). The geophysical studies provide the geotechnical information required in the engineering design in order to enhance the strength and stability of buildings or structures. The applications of such geophysical investigations are used for the determination of depth to bedrock, structural mapping and evaluation of subsoil competence (Burland and Burbidge, 1981; Burger, 1992). The use of electrical resistivity imaging to address a wide variety of hydrological, environmental and geotechnical problems is increasingly becoming very popular. The 2D electrical resistivity imaging is now being used to detect fractures and cavities in the subsurface, geotechnical investigations for buildings, roads, bridges and dams. The method can also be used for delineating archaeological features, locating surface utilities and for monitoring pollution seepage through the earth's subsurface. The method has been proven to be an effective tool for indentifying anomalies and defining the complexity of the subsurface geology (Griffiths and Barker, 1993; Loke and Barker, 1996a; Giano et al., 2000; Ugwu, 2012; Andrews et al., 2013). The 2D electrical resistivity imaging in which the subsurface is assumed to be varying vertically down and laterally along the direction of profile but constant in the perpendicular direction has been used to investigate areas with moderately complex geology (Griffiths and Barker, 1993; Andrews et al., 2013).

The electrical imaging or electrical tomography is a survey technique recently developed for the investigation of areas of complex geology where the use of resistivity sounding and other

techniques are unsuitable (Griffiths and Barker, 1993). It involves measuring a series of constant separation traverses with the electrode spacing being increased with each successive traverse. Since increasing separation leads to greater depth of penetration, the measured apparent resistivities may be used to construct a vertical contoured section displaying the variation of resistivity both laterally and vertically over the section. Electrical resistivity tomography has also been found to be a time saving and more accurate subsurface modelling technique. 2D survey measures the resistivity changes both in the vertical direction, as well as in the horizontal direction along a common survey line at the same time. 2D electrical imaging doesn't only give more accurate results and save time, it is also cost effective. 2-D imaging survey involves about 100 to 1000 measurements.

## **1.2 Location of the Study Area**

Barnawa is situated within the Basement Complex rock of Northwestern Nigeria with variable overburden thickness (Figure 1.1). The area is bounded by latitudes  $10^{\circ} 25' 28''$ N and  $10^{\circ} 35' 53''$  N and longitudes  $7^{\circ} 21' 49''$ E and  $7^{\circ} 30' 00''$  E. The study area is located at Barnawa-Narayi junction, Barnawa, Kaduna, Kaduna State (Figure 1.2). The terrain is relatively flat and accessible by road.

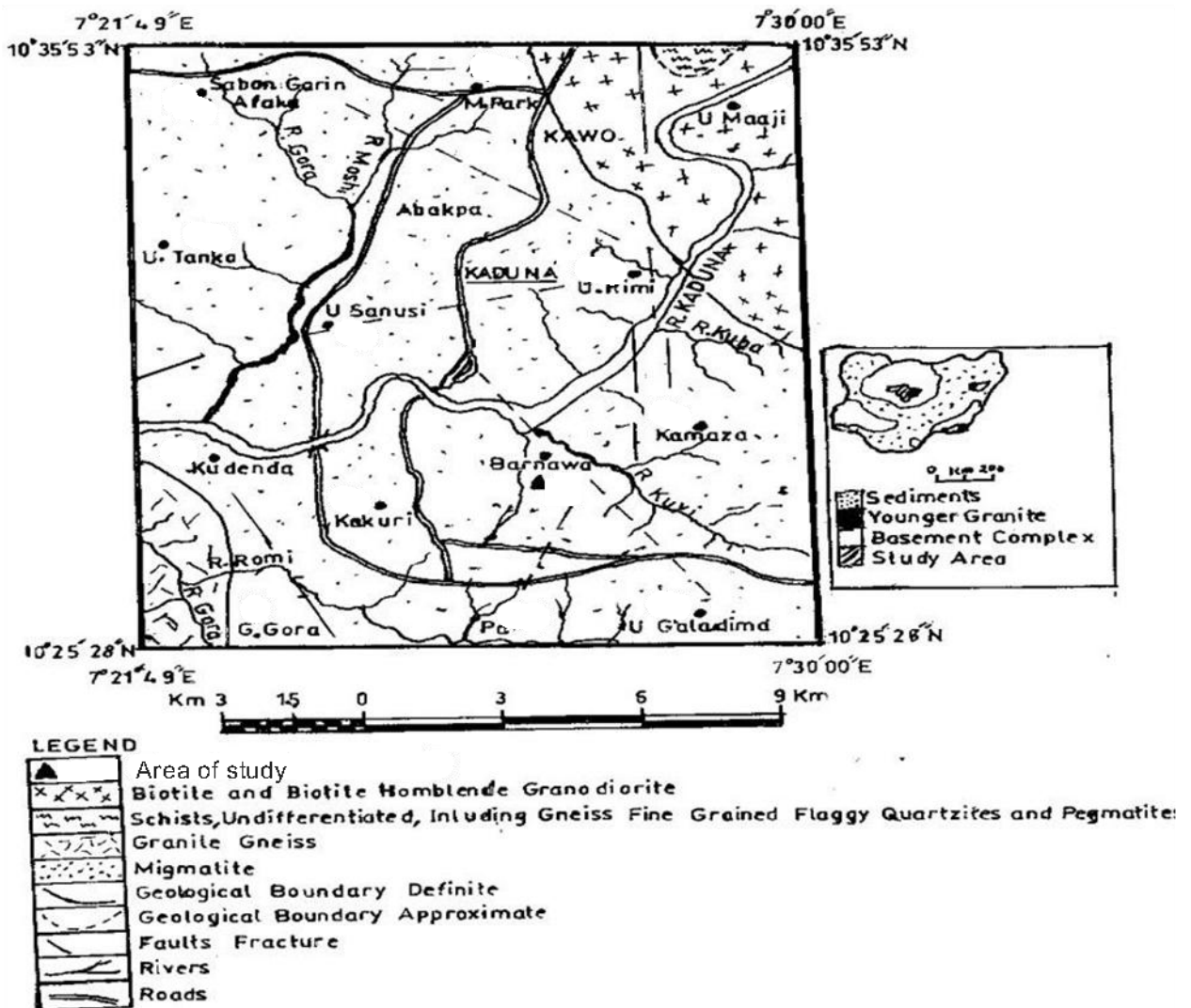


Figure 1.1: Geological map of some parts of Kaduna town showing Barnawa which is the Study Area (After Jatauet al., 2013)



**Figure 1.2: Google Image of the Study Area (Barnawa)**

### **1.3 Aim and Objectives**

The aim of the study is to carry out a geophysical investigation to find out why the buildings at Barnawa-Narayi junction are collapsing. The objectives are therefore:

- i. to determine the presence of faults, fractures, voids and clay that may pose danger to the existing structures;
- ii. to determine the depth to the bedrock within the area of study and
- iii. to obtain the thickness of the weathered basement distribution within the area of study.

### **1.4 Justification of the Study**

Due to the collapse of buildings in the study area, there is a need to provide information on the subsurface sequence and structural disposition necessary for the buildings. Detailed geophysical investigation provides such information.

Since no reported subsurface investigation has been done in the area of study, this work shall provide the following results; the possible presence of faults, fractures, voids and clay that may pose danger to the existing structures, depth to bedrock and thickness of weathered basement (aquiferous zone).

## CHAPTER TWO

### LITERATURE REVIEW

#### 2.1 Previous Geophysical and Geological Investigations in the Study Area

Abdullahiet al., (2014) carried out geoelectrical method in the evaluation of groundwater potential and aquifer protective capacity of overburden units around Sabo area in Kaduna State, Northwestern Nigeria. Their results delineated three to five geoelectric sections in the study area, namely: the topsoil (which consists of lateritic clay), river sand and gravel, clayey sand, weathered transition zone/ fractured layer and the fresh basement. The weathered and fractured basement rocks constitute the aquifers or aquiferous zones in the area with the weathered basement as the more prominent. These aquifers are characterized by thick overburden found within the basement depressions with maximum value of 65m and resistivity values between 10 $\Omega$ m and 756 $\Omega$ m.

Jatauet al., (2013) carried out Groundwater Investigation in Parts of Kaduna South and Environs using Wenner Offset Method of Electrical Resistivity Sounding. Their research revealed a four layer case for Barnawa area with topsoil being sandy clay with thickness of 1.7m and resistivity value of 216 $\Omega$ m. The second layer composed of lateritic clay has a thickness of 2.4m and resistivity value of 202 $\Omega$ m. The third layer, probably a weathered layer or fractured basement with resistivity value and thickness of 115 $\Omega$ m and 14.4m respectively and is underlain by fresh basement with resistivity value of 1931 $\Omega$ m.

Adukwu and Fadele (2012) worked on the Relevance of Geophysics in Foundation Evaluation in a Typical Basement Complex of Northwestern Nigeria. The Vertical Electrical Sounding (VES) results

revealed heterogeneous nature of the subsurface geological sequence. The geologic sequence beneath the study area is composed of top soil (clayey and sandy-lateritic), weathered layer, partly weathered or fractured basement and fresh basement. The resistivity value for the topsoil layer varies from  $7\Omega\text{m}$  to  $361\Omega\text{m}$  with thickness ranging from 1.19m to 3.90m. The weathered basement has resistivity values ranging from  $60\Omega\text{m}$  to  $336\Omega\text{m}$  and thickness of between 0.60m and 11.40m. The fractured or partly weathered basement has resistivity values ranging from  $442\Omega\text{m}$  to  $987\Omega\text{m}$  and thickness of between 4.61m and 19.50m. The fresh basement has relatively high resistivity values ranging from  $967\Omega\text{m}$  to  $6036\Omega\text{m}$  with infinite depth. However, the depth from the earth's surface to the bedrock surface varies between 2.29m to 20.80m. Based on the resistivity values, it was concluded that the subsurface material upto the depth greater than 15m was competent and had high load-bearing capacity. However, resistivity values less than  $50\Omega\text{m}$  at depths of 5m to 10m indicate highporosity, high clayey sand content and high degree of saturation which are indications of soil conditions requiring serious consideration in the design of massive engineering structures.

Fadeleet al.,(2012) carried out Engineering Geophysical Investigation Around Ungwan Doka, Shika Area within the Basement Complex of Northwestern Nigeria. The geoelectric section revealed two to four lithologic units defined by the topsoil, which comprised clayey-sandy and sandy lateritic hard pan; the weathered basement; partly weathered/fractured basement and the fresh basement. The resistivity values range from  $26\Omega\text{m}$  -  $373\Omega\text{m}$ ;  $77\Omega\text{m}$  -  $391\Omega\text{m}$ ;  $473\Omega\text{m}$  -  $708\Omega\text{m}$  and  $1161\Omega\text{m}$  -  $3600\Omega\text{m}$  in the topsoil, weathered, fractured basement and fresh basement respectively. Layer thicknesses vary from 0.38m – 6.58m in the topsoil, 1.10m – 33.04m in the weathered layer and 5.86m – 34.10m in the fractured basement. Depth from the surface to bedrock/fresh basement generally varied between 2.65m and 37.75m. Based on the resistivity values, it was concluded that the subsurface material up to the depth of 25m was competent and has high load-bearing capacity.

However, resistivity values less than  $100\Omega\text{m}$  at depths of 10m-15m indicate high porosity, high clayey sand content and high degree of saturation which are indications of soil conditions requiring serious consideration in the design of massive engineering structures.

Aboh (2009) carried out an assessment of the aquifers in some selected villages in Chikun Local Government Area, Kaduna State, Nigeria. The result of the interpreted VES data suggests that the area is underlain by three to five layers. The geologic sections derived from the analyzed geoelectric section suggest that the alluvial deposits of sand, silt and sandy clay as well as the weathered and fractured basement rocks constitute the aquifer in the areas. The average thickness of the aquifer was found to be 25m. The geoelectric sections generated also suggest that the resistivity values of the aquifer components range from  $100\Omega\text{m}$  to  $250\Omega\text{m}$  for the alluvial deposits to an average of  $50\Omega\text{m}$  to  $350\Omega\text{m}$  for the weathered/fractured basement formations. The analysis of these sections obtained for this work suggests that the storage elements for ground water in these selected villages in Chikun LGA consists of mainly the weathered basement and fractured basement rocks of the Precambrian Basement Complex. It was found that the weathered basement aquifers are characterized by resistivity values in the range of  $80\Omega\text{m}$  to  $56\Omega\text{m}$  while resistivity values of  $53\Omega\text{m}$  to  $456\Omega\text{m}$  are associated with the aquifers of the fractured basement rocks.

Alheri and Jatau (2009) carried out a geophysical survey to determine the Weathered Regolith using Seismic Refraction method in parts of Kaduna South Industrial Area. They concluded from the research that the area had three to four layers, and that the borehole log of the study area revealed the same geologic unit with their research.

Chiemeke and Osazuwa (2007) worked on the Application of Seismic Refraction Tomography for Subsurface Imaging in central northern Nigeria. Their research showed that seismic refraction tomography can be used to image the subsurface to delineate the various strata within the subsurface, the weathered basement and depth to basement. The lithology analysis revealed that the top soil is made up of laterite and silty clay. The main aquifer is made up of the weathered basement, pebbles and gravels while the fresh basement is composed of granite and quartzites occurring with gneisses. The results of the study showed that the thickness of the overburden within the survey area is about 10.05m. The thickness of the weathered basement is about 7.04m. Hence, the depth to the fresh basement is about 17.09m.

## **2.2 General Geology of the Study Area**

The study area lies within the Basement Complex of Nigeria (Figure 2.1). The Basement Complex includes all rocks older than the late Proterozoic (McCurry, 1976), and is composed mainly of gneisses, migmatite, granites and some extensive areas of schist, phyllites and quartzites (Preeze and Barber, 1965; Baimba, 1978).

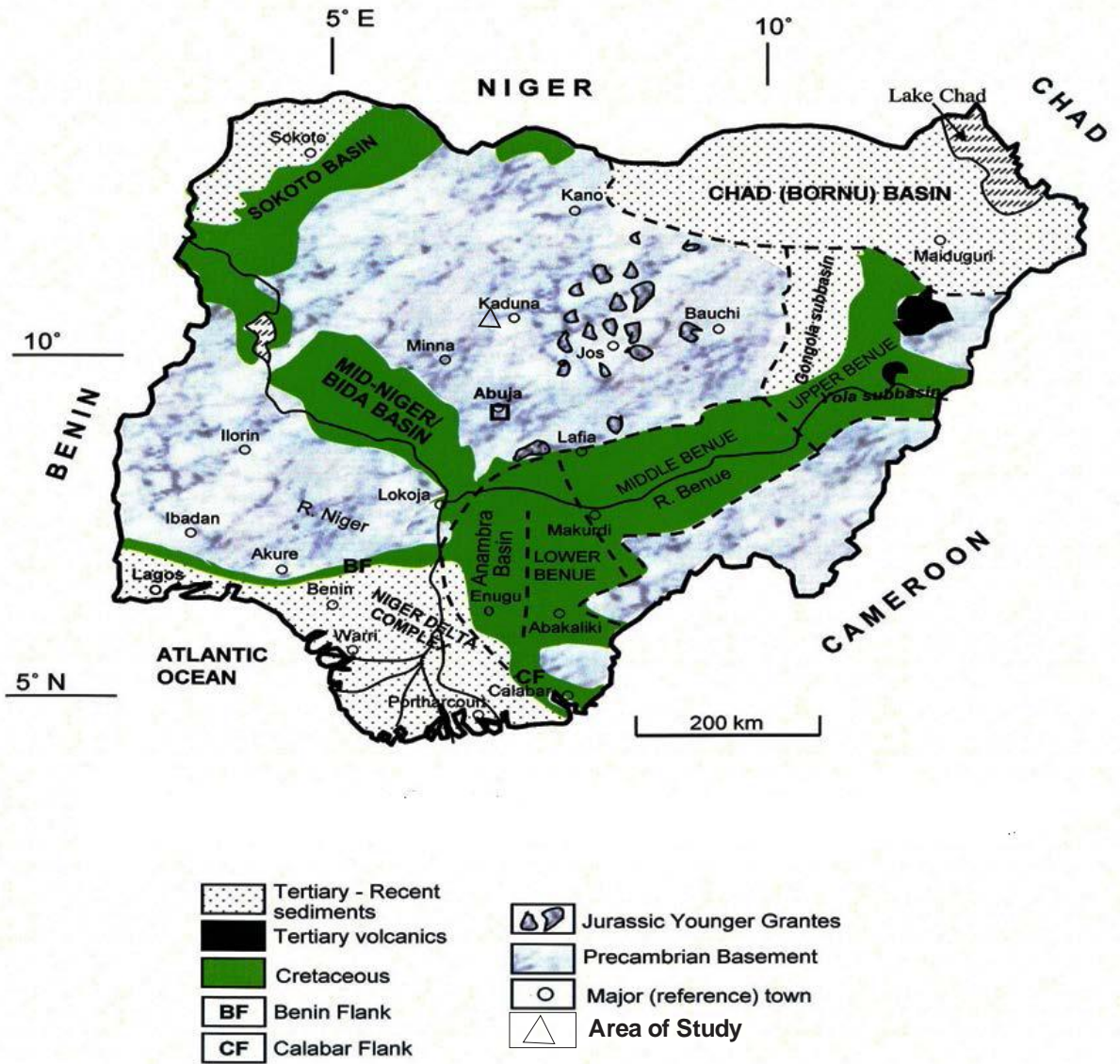


Figure 2.1: Basement geological map of Nigeria showing the Study Area (After [Obaje, 2009](#))

According to McCurry (1976), the whole Basement Complex has been through at least two Tectonic-metamorphic cycles and consequent metamorphism, migmatization and granitisation have extensively modified the rocks so that they generally occur as relict rafts and xenoliths in migmatite and granites. Two groups of granites are present and these are the Older Granites and the Younger Granites. The Older Granites are widespread and often give rise to smoothly domed hills which typically rise to about 170m above the surrounding plains (Russ, 1957). The Younger Granites which include granites, syenites and rhyolites cover extensive areas in the Plateau province but there are also smaller masses in Southern Kaduna, Kano, Bauchi and Zaria provinces and some other isolated masses in the Borno province (Russ, 1957). Their rocks are hard, with low permeability and generally not water-bearing. The rocks are aquifers only when they are either weathered or fractured, otherwise they are dry or at best contain just little amount of water (Olabode et al., 1999). Over most of the area underlain by the Basement Complex, there is a thin discontinuous layer of weathered rocks, mostly pronounced where the topography is subdued. The average thickness of the layer is probably of the order of 15m, but in some areas it may extend to a depth of upto 60m (Russ, 1957). The actual depth of the weathered zone depends on the length of time in which the rocks have been exposed to surface or near surface conditions and its original minerals. The interface between weathered and unweathered rocks is usually sharp. Weathering tends to be particularly well developed along fissure systems, which allow deep percolation of the weathering agents principally oxygenated water. River systems can sometimes be the guide to fault lines and associated fissure systems because they represent lines of weakness for erosion and weathering (Olabode et al., 1999).

## CHAPTER THREE

### METHODOLOGY

#### 3.1 Introduction

In geoelectrical resistivity tomography (near-surface), a large number of electrodes are inserted into the ground and a computer-based system scans the whole array, thus realizing a combined sounding and profiling. If the target in a proposed survey area is narrow and extends over a long distance (the 2D case), the technique effectively investigates a series of depth range on a profile line, resulting in a pseudosection of apparent resistivities. Tomographic surveys normally employ arrays of electrodes on the surface of the ground for data collection. The survey technique involves measuring a series of constant separation traverses with the electrode separation being increased with each successive traverse. Since increasing separation leads to information from greater depth, the measured apparent resistivities may be plotted as a contoured section, which reflects qualitatively the spatial variation in resistivity in the vertical cross-section. Length of profile, depth of penetration and resolution required determine the unit electrode spacing.

#### 3.2 Fieldwork

The fieldwork was accomplished between 3rd of April and 10th of April, 2014, before the start of the rainy season. This period was chosen for the fieldwork, to avoid disturbance by rain which would slow down the work.

Electrical resistivity imaging using Schlumberger array was used along the seven (7) profiles. A direction of SE-NW azimuth was employed in profiles 2,4,5,6 and 7 and a W-E azimuth in profiles 1 and 3 in the orientation of the profiles (Figure 3.1).

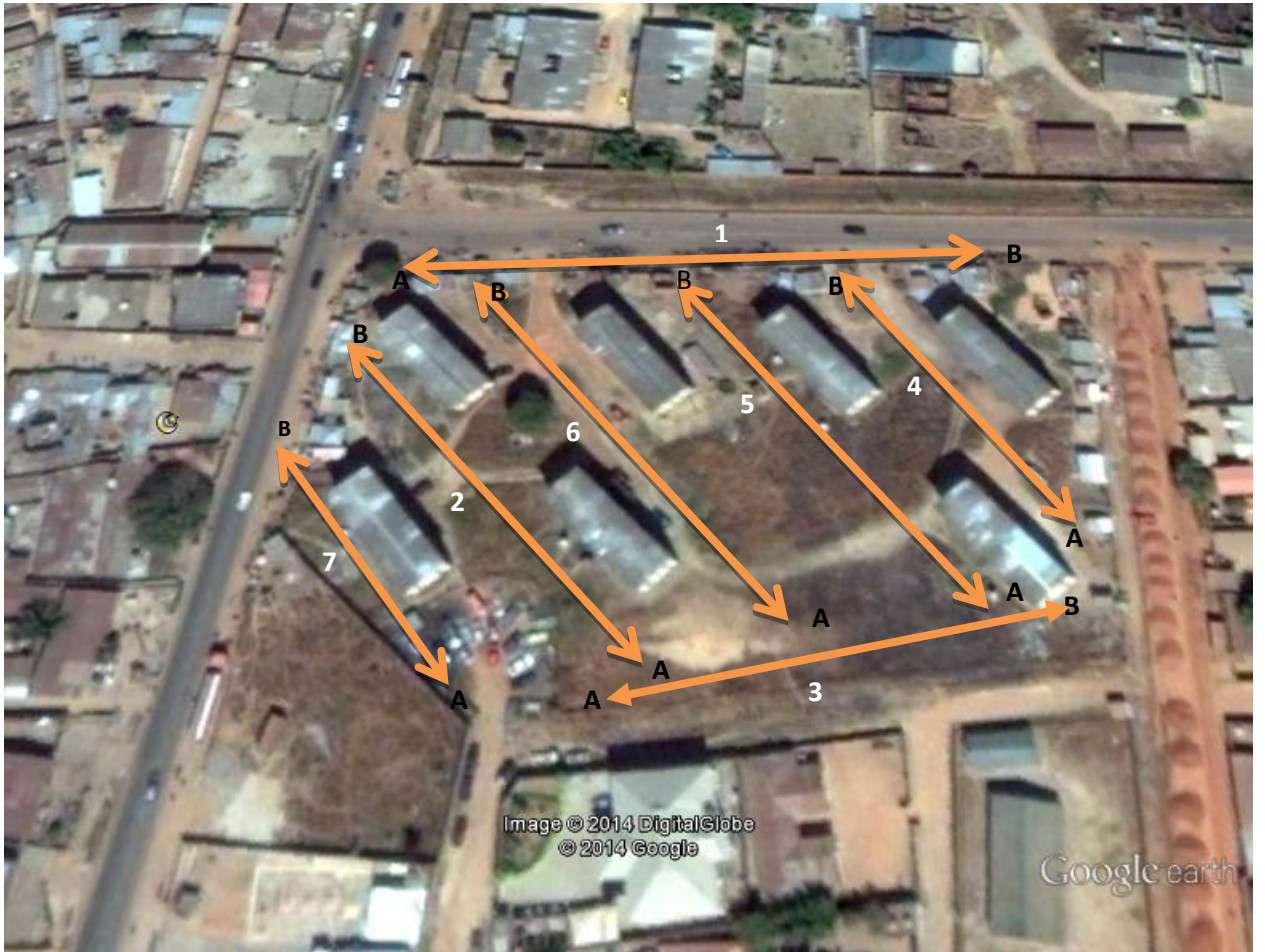


**Figure 3.1: Google Image of Study Area Showing Profiles 1 to 7**

### **3.3 Choice of the method**

Schlumberger electrode layout was used, for the following reasons:

The smaller separation of the potential electrodes (Figure 3.2) reduces noise due to ground current which may limit the useful depth of penetration.

It also provides a better horizontal coverage (Figure 3.3), and the maximum depth of penetration of this array is about 15% larger than the Wenner array (Loke, 2000).

### **3.4 Field Procedure**

Electrical Resistivity Tomography (ERT) is a method by which 2D images of subsurface resistivity distribution are generated. Using this method, features with electrical properties differing from those of the surrounding material may be located and characterized in terms of electrical resistivity, geometry and depth of burial. The electrical resistivity tomography data were collected using computer-controlled measurement systems connected to multi-electrode arrays. The data acquisition process is completely controlled by the computer software which checks that all the electrodes are connected and properly grounded before measurement starts. After adequate grounding is achieved the software scans through the measurement protocol selected. The Schlumberger array was chosen for this survey. The Terrameter SAS 1000, Electrode Selector ES 464, stainless steel electrodes, cable jumpers or electrode connectors, cables and reels, hammers, external 12 volts battery which was charged to full capacity before going to the field, spare

batteries and a field umbrella were conveyed together with the members of the field team to the site of this research for commencement of the geophysical investigation.

The two electrode cables 1 and 2 depending on the current position along the line of survey were rolled out in the direction of the profile, with the cable reel end facing the highest coordinates. Each cable has 21 take-outs.

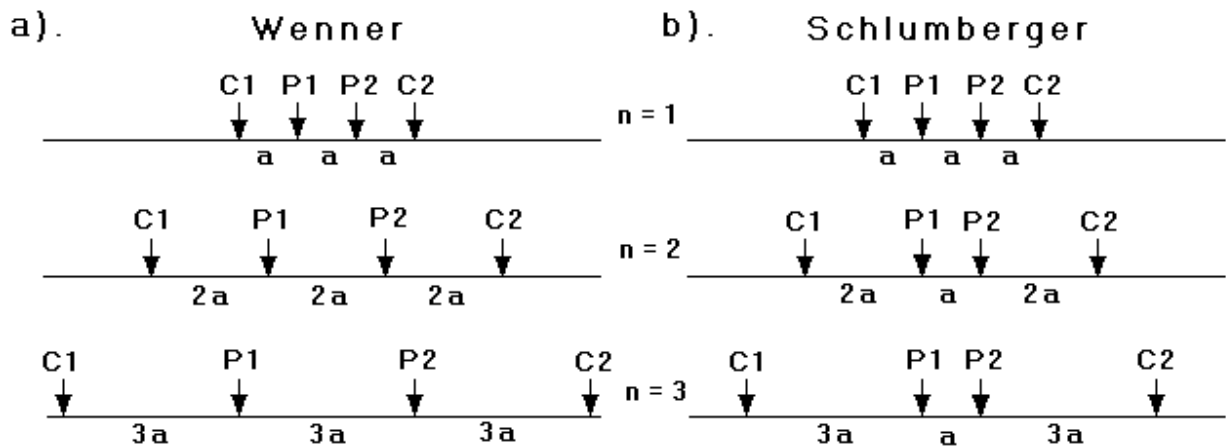
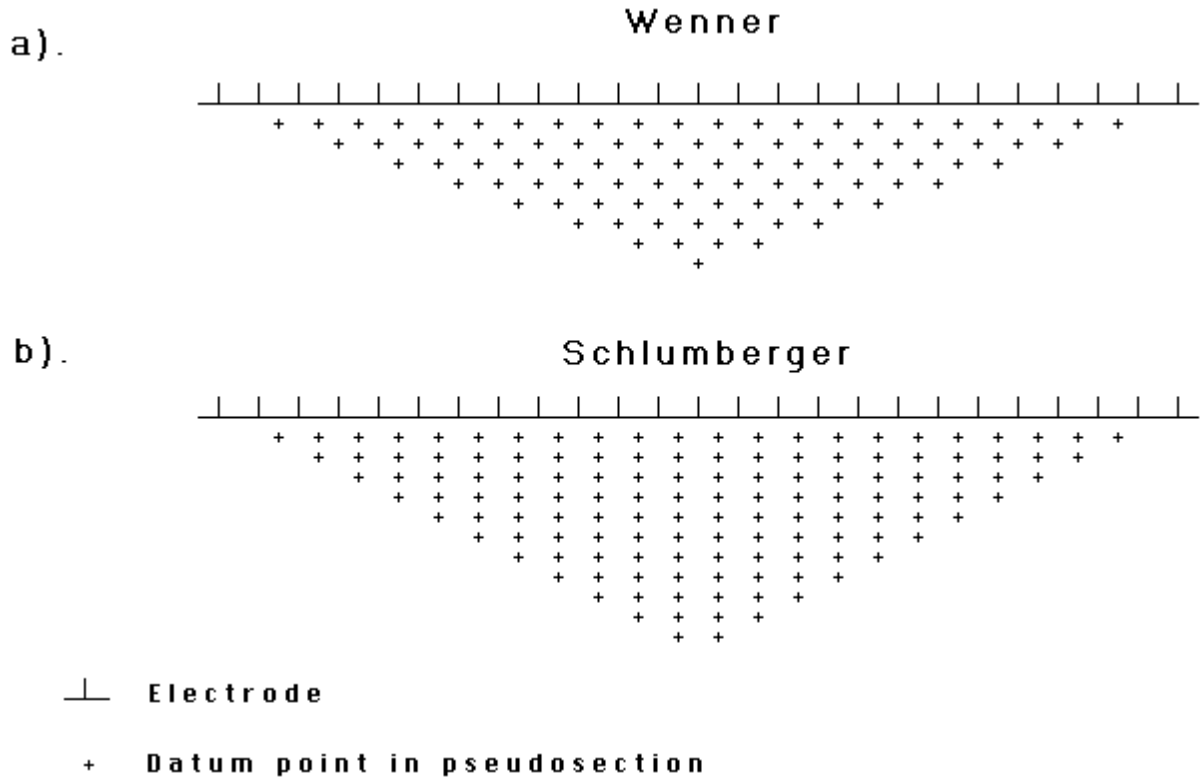


Figure 3.2: The steps used to increase the depth of investigation by (a) Wenner and (b) Schlumberger arrays.



**Figure 3.3: Arrangement of data points in the pseudosections for (a) Wenner array and (b) Schlumberger array.**

The Terrameter SAS 1000 and the ES 464 were placed at the centre of the layout. The two cables were connected to the ES 464 at the centre of the cable spread. The serial port of the Terrameter was connected to the Electrode Selector. The electrodes were connected to all the take-outs at intervals of 2m on the cables using cable jumpers. For moist or soft ground, electrodes were just pushed into the ground by hand and then connected. However, hammering and wetting were done on dry and hard ground. The Terrameter was then connected to an external 12 volts battery and switched on, which automatically switched on the Electrode Selector and the system set-up was echoed on the screen. The instrument was set to resistivity mode and LUND Imaging System was selected. Electrode test was commenced immediately and grounding improved for the electrodes with bad ground contact. The connectors were also checked for unsatisfactory electrode positions. Electrodes were tested

pair-wise against each other starting from the outermost electrodes going towards the centre. The electrode test checks if it is possible to transmit current through all electrodes. This test takes a couple of minutes but saves time afterwards because the programme may stop depending on poor electrode contact. Measurement may also stop if the batteries for either the Terrameter or the Electrode Selector are low. The programme automatically continues to measure using the two electrode cables when the contact is satisfactory. It was ensured that measurements did not stop during the measurement period. As measurement continued, apparent resistivity values were echoed on the screen. When measurements on each layout finished, the programme was stopped and the Terrameter switched off. The cables were disconnected, wound up, and the electrodes and cable jumpers were all collected together. The instrument was then transferred to a new profile and the entire process repeated until all the profiles were completed. While measuring the profiles, the positions of reference points along the lines were noted. The coordinates of the midpoints along the profiles were noted to facilitate identification of points for further investigation (Table 3.1). Seven profiles were used. Electrode spacing of 2m and 42 electrode systems were utilized which sums the total length covered to be 84m. Resistivity inverted models were computed using RES2DINV software. The resistivities of the blocks were adjusted and iterated until the calculated and field apparent resistivities agreed to the bearest minimum differences (Loke, 2000).

**Table 3.1: Coordinates of midpoints along the profiles.**

Profile	Latitude	Longitude
1	N10°28'.5943"	E7°26'.678"
2	N10°28'.5705"	E7°26'.514"
3	N10°28'.543"	E7°26'.785"
4	N10°28'.5842"	E7°26'.1103"
5	N10°28'.5757"	E7°26'.905"
6	N10°28'.7350"	E7°26'.1716"
7	N10°28'.6607"	E7°26'.1953"

### 3.5 Typical Resistivity Values of Earth Materials

Of all the physical properties of earth materials (rocks and minerals), electrical resistivity has the widest range of variation. Resistivity of metallic minerals may be as small as  $10^{-5}\Omega\text{m}$ . That of dry close-grained rocks like gabbro could be as large as  $10^7\Omega\text{m}$ . The maximum possible range is even greater, from native silver,  $1.6 \times 10^{-8}\Omega\text{m}$  to pure sulphur  $10^{16}\Omega\text{m}$ . A good conductor is usually defined as a material of resistivity less than  $10^{-5}\Omega\text{m}$  while an insulator is one having resistivity greater than  $10^7\Omega\text{m}$  and between this limit lies the semi-conductors (Telford et al., 1990). The common minerals forming rocks and soils have very high resistivity values in dry condition and the resistivity of rocks and soils is therefore normally a function of the amount and quantity of water in pores and fractures. The degree of connection between cavities is also important; consequently the resistivity of a rock type or soil type may vary widely. The electrical resistivity varies between different geological materials depending mainly on variations in water content and dissolved ions in the water. Resistivity investigations can thus be used to identify zones with different electrical properties, which can then be referred to different geological strata. However, the variation may be limited within confined geological area and variations in resistivity within certain soil or rock type will reflect variations in physical properties. For example the lowest resistivities encountered for sandstones and limestone mean that the pore spaces in the rock are saturated with water, whereas the highest values represent strongly consolidated sedimentary rock or dry rock above the groundwater surface. Sand, gravel and sedimentary rocks may also have very low resistivities provided the pores in the rocks are saturated with saline water. Fresh crystalline rock is highly resistive apart from certain ore minerals, but weathering commonly produces highly conductive clay rich saprolite. The variation in

characteristics within one type of geological material makes it necessary to calibrate resistivity data against geologic documentation for instance, surface mapping, test pits or drilling. Typical ranges of resistivities of geologic materials are shown in Figures 3.4 and 3.5. The amount of water in a material depends on the porosity, which may be divided into primary porosity and secondary porosity. Primary porosity consists of pore spaces between the mineral particles and occurs in soils and sedimentary rocks. Secondary porosity consists of fractures and weathered zones, and this is the most important porosity in crystalline rocks such as granites and gneisses. Secondary porosity may also be important in certain sedimentary rocks such as limestone. Even if the porosity is rather low, the electrical conduction taking place through water filled pore spaces may reduce the resistivity of the material drastically. The degree of water saturation will of course affect the resistivity, thus the resistivity above the groundwater level will be higher than below if the material is the same. Consequently, the method can be used to find the depth to groundwater in materials where a distinct groundwater table exists. However, if the content of fine grained material is significant, the water content above the groundwater surface, held by hygroscopic and capillary forces may be large enough to dominate the electrical behaviour of the material. The resistivity of pore water is dominated by the concentration of ions in solution, the type of ions and the temperature. The presence of clay minerals strongly affects the resistivity of sediments and weathered rocks. The clay minerals may be regarded as electrically conductive particles which can absorb and release ions and water molecules on its surface through an ion exchange process. Very roughly, igneous rocks have the highest resistivity, sedimentary rocks the lowest and metamorphic rocks intermediate. However, there is a considerable overlapping. Resistivities of particular rock types vary with age and lithology, since the porosity of the rock and the salinity of the contained water are affected by both.

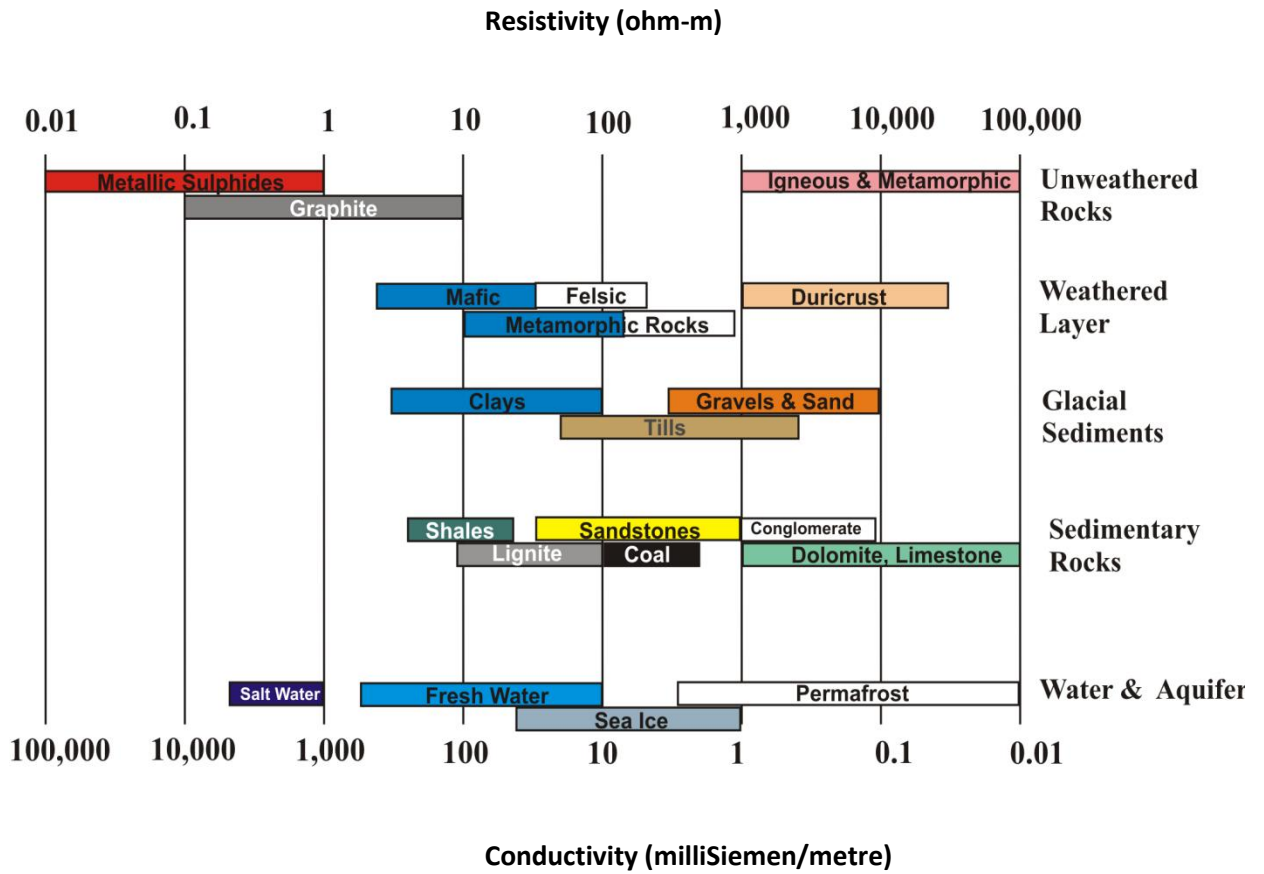


Figure 3.4: A Typical Range of Resistivities of Geological Materials (ABEM Instruction Manual, 2010).

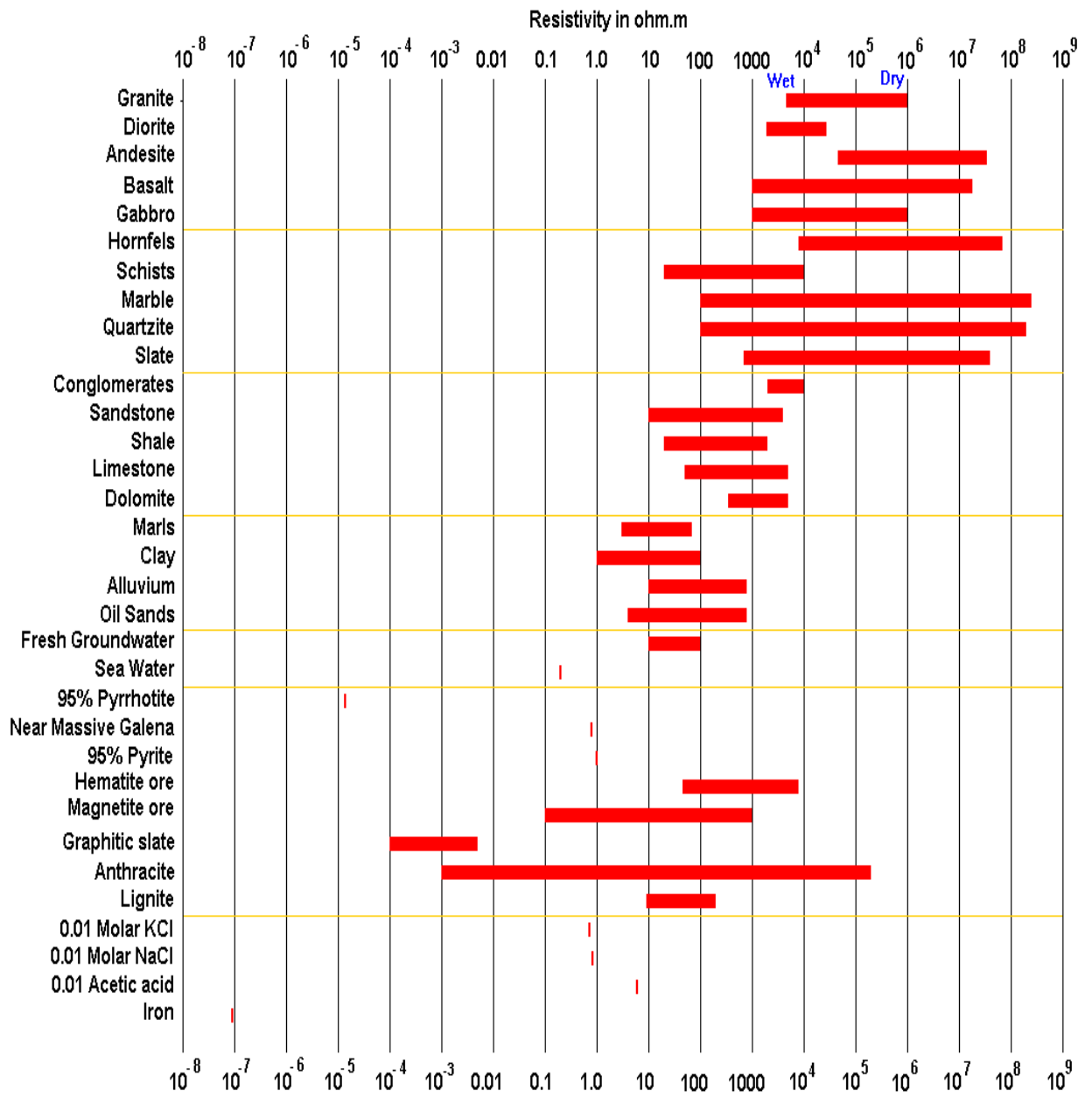


Figure 3.5: Resistivities of Rocks, Soils and Minerals(Loke, 2004)

For example the resistivity range of Precambrian volcanic is  $200\Omega\text{m} - 5000\Omega\text{m}$  while for quaternary rocks of the same kind is  $10\Omega\text{m} - 200\Omega\text{m}$  (Telford et al., 1990). As the variation in temperature of the ground is generally small, the temperature influence is normally negligible.

However, in geothermal applications the variation could be significant even in permafrost regions. The mobility of ions increases with increasing temperature as the viscosity of water is lowered. Hence, a decrease in resistivity with increasing temperature can be observed for materials where electrolytic conduction dominates.

### **3.6 Theory of Direct Current Resistivity Method**

This method is based on the fact that when an electric current is driven into the earth, any variation of the subsurface resistivity will alter the current flow, which will in turn affect the distribution of the electric potential. The measurement of the electrical potential and current on the earth's surface will make it possible to obtain information about the resistivity variation of the subsurface in the area concerned (Telford et al., 1990). The electrical resistivity method is one of the most relevant geophysical methods applied in environmental studies in basement terrains. In groundwater studies for instance, the relevance of the method is based on the usually significant resistivity contrast between the weathered zone and/or fractured column which contains the water and the resistive fresh bedrock. There is a considerable variety of resistivity methods all of which employ artificial source of current which is introduced into the ground through point electrodes or long line contacts. The resulting potential established in the earth is measured at other electrodes in the vicinity of the current flow. The current is noted; hence it is possible to determine the apparent resistivity of the subsurface. In this regard, the resistivity method is the most superior; at least theoretically, to all other electrical methods since quantitative results can be obtained by using a controlled source of

specific dimensions (Telford et al., 1990). Direct current (D.C.) or an alternating current (A.C.) of low frequency is used and the method is often called D.C. resistivity method. In this method, an electric current is introduced into the ground by means of two current electrodes, which set up a stationary current field, and because of the Ohmic potential drop, an electrical potential field is also created. This field gets distorted in the neighbourhood of a subsurface zone of anomalous conductivity, and the aim is to search for such anomalous zones in the electrical field with a pair of potential electrodes. The assumption made here is that the current flow in the potential measuring circuit is negligible compared with the current flow in the ground, so that the potential electrodes themselves will have no disturbing effect upon the electrical field (Grant and West, 1965). Schlumberger array (Figure 3.6) was adopted for the survey. A and B are point current electrodes through which current is driven into the ground, while M and N are two potential electrodes to record the potential distribution in the subsurface within the two current electrodes. From Ohm's law, the current I and potential U in a metal conductor at constant temperature are related as follows:

$$U=IR \tag{3.1}$$

where R is the constant of proportionality termed resistance and it is measured in ohms. The resistance R, of a conductor is related to its length L and cross sectional area A by;

$$R=\frac{\rho L}{A} \tag{3.2}$$

where  $\rho$  is the resistivity and it is a property of the material considered. From equations (3.1) and (3.2),

$$U=\frac{I\rho L}{A} \tag{3.3}$$



Schlumberger array involves fixing the potential electrodes at points M and N, and symmetrically increasing the current electrode separation AB about the centre by displacing A and B outwardly in steps. This will increase the depth of penetration within the separation AB. Thus, the varying resistivity measured when electrode array position is varied in an inhomogeneous medium is termed apparent resistivity. For simple treatment, a semi-infinite solid with uniform resistivity,  $\rho$ , is considered. A potential gradient is measured at M and N when current electrodes located on the surface of the equipotential surface is semi-spherical downwards into the ground at each electrode. The surface area will then be  $2\pi L^2$ , where L is the radius of the sphere. Thus,

$$U = \frac{I\rho}{2\pi L}$$

(3.4)

By deduction then, the potential at M ( $U_M$ ), due to the two current electrodes, is

$$U_M = \frac{I\rho}{2\pi} \left( \frac{1}{r_1} - \frac{1}{r_2} \right) \tag{3.5}$$

Similarly, the potential at electrode

N ( $U_N$ ) is given by

$$U_N = \frac{I\rho}{2\pi} \left( \frac{1}{r_3} - \frac{1}{r_4} \right)$$

(3.6)

where  $r_1$ ,  $r_2$ ,  $r_3$  and  $r_4$  are shown in Figure 3.6.

The potential difference,  $\Delta U$ , across electrodes M and N is  $U_M - U_N$ . If the body is inhomogeneous like the study area, apparent resistivity ( $\rho_a$ ) is considered,

$$\rho_a = K \left( \frac{\Delta u}{I} \right) \quad (3.7)$$

where  $\rho_a$  is apparent resistivity in ohm-metre, and

$$K = 2\pi \left[ \frac{1}{\left( \frac{1}{r_1} - \frac{1}{r_2} \right) - \left( \frac{1}{r_3} - \frac{1}{r_4} \right)} \right] \quad (3.8)$$

K is called the geometric factor whose value depends on the type of electrode array used. For Schlumberger array, if  $MN = 2b$  and  $\frac{AB}{2} = L$  then,

$$K = \pi \left( \frac{L^2}{2b} - \frac{b}{2} \right) \quad (3.9)$$

### 3.7 Principle of Lund Resistivity Imaging and Instrumentation

Tomography is defined as an imaging technique, which generates a cross sectional picture (tomogram) of an object by utilizing the object's response to the non-destructive, probing energy of an external source. Electrical Resistivity Tomography (ERT) is a method by which two dimensional (2D) images of subsurface resistivity distribution are generated (Batayneh, 2006). Electrical Resistivity Imaging (tomography) involves measuring a series of constant separation traverses with the electrode spacing being increased with each successive traverse. Thus, 2D resistivity imaging requires data to be recorded with different electrode separations along a traverse line. It is important to have

enough data to cover laterally and in terms of electrode separations to recover complex structures in the ground and thus demands the use of automated multi-electrode data acquisition systems to be practicable. The Schlumberger spread was used for this survey. The basis of the LUND Resistivity Imaging technique follows from that of the normal resistivity technique, in which case when current is driven into the earth, any variation of the subsurface resistivity will alter the current flow which will in turn affect the distribution of the electrical potential. Buried bodies distort the regular pattern of current flow.

A conductive body concentrates electric current flow lines towards itself, while a resistive body causes the current to flow around itself. The potential fields are hence deflected and their deflections can be detected using potential electrodes at the surface of the earth. Thus, from the measurements on the earth's surface of the electrical potential and the current, it is usually possible to obtain information about the variation of the subsurface resistivity. Sand, fine grained sediments and bedrock are expected to exhibit large contrasts in electrical resistivity hence the electrical resistivity method should be well suited to resolving them. When the resistivity values are correlated with different types of geologic materials, they can provide useful information for interpretation.

For resistivity measurement nowadays, there is a range of instrumentation from very simple to highly sophisticated equipment with the latter including a computer for infield data processing. The basic parts of any resistivity instrumentation are a portable power source which is either D.C. or low frequency A.C., electrodes, preferably stainless steel electrodes, cables and reels, and meters for measuring current and voltage both of which may be combined in a single meter reading resistance. With the development of computer-controlled data collection and also automatic data inversion, the use of computer-controlled multi-electrode systems with automatic data measurements and data

quality control for the data acquisition allow a dramatic increase in field productivity. Such is the ABEM LUND Imaging System.

### **3.8 The ABEM Lund Imaging System**

The LUND Imaging System is a multi-electrode system for cost effective and high resolution 2D and 3D resistivity surveys. It is an automatic electric imaging system suited for automatic resistivity profiling and drilling. The LUND Resistivity Imaging System consists of a basic unit, a standard resistivity meter (ABEM Terrameter SAS1000) and a multi-channel relay matrix switch unit called Electrode Selector ES 464. The system also has four multi-conductor electrode cables wound on reels each with 21 take-outs, stainless steel electrodes and cable jumpers and various connectors. The system is compatible with a portable PC-type computer or note book (laptop).

Data acquisition includes software featuring automatic measuring process, in-field quality control of measurements, automatic roll along, electrode cable geometry and switching sequence defined in address and protocol files which allow user defined survey strategies and arrays, onscreen echo of measurement progress, software for graphical and depth interpretation including pseudosection plotting in gray scale or colour. Model section plotting of 1D and 2D model interpretation sections in colour or gray scale including topography, reference data and reference levels, utility software for extraction of VES, data manipulation and conversion, graphical output in PCX-file format etc, are also available (ABEM LUND Instruction Manual). The Lund ES 464 basic system includes one ES 464 field unit with clip-on NiCd rechargeable battery pack and one communication cable from electrode selector to Terrameter. It is light weight and has waterproof, rugged cast Aluminium casing. The Terrameter SAS system consists of a basic unit called the Terrameter SAS 1000 and accessories like ES 464. Signal Averaging System (SAS) is a method whereby consecutive readings are taken

automatically and the results are averaged continuously. Signal Averaging System (SAS) results are more reliable than those obtained from single-shot systems. The SAS 1000 can operate in different modes, e.g., resistivity, self potential and induced polarization. The SAS 1000 is powered by a clip-on NiCd battery pack or by an external 12 volts source, which clips conveniently onto the bottom of the instrument. The SAS-EBA external 12 volts adapter allows the Terrameter to utilize an external 12 volts D.C. source, e.g., a car battery (ABEMLUND Instruction Manual). Stainless steel electrodes establish electric contact between electronic conductors, which are long cables, to an ionic conductor which is the ground. Electrodes generate noise, which is only at the potential electrodes. Noise is the fluctuating voltage that appears between a pair of electrodes placed so close that no other natural voltages appear. But stainless steel electrodes create less noise. Current electrodes and potential electrodes make good contact with the ground to ensure low contact resistance and stability respectively (ABEM Instrument AB, 2010). The cables incorporate heavy gauge conductors with excellent insulation to ensure good survey results. The cables are expandable for deeper penetration by connecting them in series with a cable joint. The cables have take-outs at 2m intervals from which they are connected to the electrodes using cable jumpers having crocodile clips at both ends. The cables are wound on reels. Figure 3.7 shows the basic instrumentation of the ABEM LUND Imaging System and accessories.



**Figure 3.7:ABEM LUND Imaging System together with Terrameter SAS 1000, ES 464 and Accessories(ABEM Instrument AB, 2010)**

## CHAPTER FOUR

### FIELD RESULTS AND INTERPRETATION

#### 4.1 Introduction

In electrical resistivity tomography (ERT), prior information about unknown parameters (such as resistivity values and depth of the layers) are of paramount importance for inversion processing (Cardarelli and Fischanger, 2006).

As in all other geophysical methods, the interpretation of data from electrical imaging involves expressing in geological terms the information obtained from the measured apparent resistivity data. Such an interpretation demands, on the one hand, considerable practical experience with the method and, on the other hand, a sound knowledge of the geology of the region under consideration. An automatic iterative method based on the smoothness-constrained least-squares method known as RES2DINV was used. This rapid 2D resistivity inversion routine considerably sharpens up the image, places the structures at approximately their correct depths and provides acceptable estimates of their true resistivities. In this work, all the available geological information on the project area was taken into consideration to constrain the interpretations. Also in interpreting the data, each layer of rock type was assumed to be homogeneous and isotropic.

#### 4.2 Data Processing

The raw field data was processed using RES2DINV (Loke and Barker, 1996b). This is a computer programme that automatically determines a two-dimensional (2D) resistivity model for the subsurface data obtained from electrical survey. It is a Window based programme. This method is based on the following equation.

$$(\mathbf{J}^T \mathbf{J} + u\mathbf{F})\mathbf{d} = \mathbf{J}^T \mathbf{g} - u\mathbf{F}\mathbf{r} \quad (4.1)$$

where  $\mathbf{F} = \mathbf{f}_x \mathbf{f}_x^T + \mathbf{f}_z \mathbf{f}_z^T$

$\mathbf{f}_x$  = horizontal flatness filter

$\mathbf{f}_z$  = vertical flatness filter

$\mathbf{J}$  = matrix of partial derivatives

$\mathbf{r}$  = a vector containing the logarithm of the model resistivity values

$u$  = damping factor

$\mathbf{d}$  = model perturbation vector

$\mathbf{g}$  = discrepancy vector

The discrepancy vector,  $\mathbf{g}$ , contains the difference between the calculated and measured apparent resistivity values. The magnitude of this vector is frequently given as a Root-Mean-Squared (RMS) value. This is the quantity that the inversion method seeks to reduce in an attempt to find a better model after each iteration. The model perturbation vector,  $\mathbf{d}$ , is the change in the model resistivity values calculated using the above equation which normally results in an “improved” model. The above equation tries to minimise a combination of two quantities, the difference between the

calculated and measured apparent resistivity values as well as the roughness (i.e. the reciprocal of the model smoothness) of the model resistivity values. The damping factor,  $u$ , controls the weight given to the model smoothness in the inversion process. The larger the damping factor, the smoother will be the model but the apparent resistivity RMS error will probably be larger. The forward problem is solved through a finite difference algorithm, whose main features are a versatile user-defined discretization of the domain and a new approach to the solution of the inverse Fourier transform.

The forward modelling subroutine is used to calculate the apparent resistivity values. The inverse procedure is based on an iterative smoothness-constrained least-squares algorithm. This computer programme uses a smoothness constrained non-linear least-squares optimization inversion technique to convert measured apparent resistivity values to true resistivity values and plot them in cross-sections. The inversion process removes geometrical effects from the pseudosection and produces an image of true depth and true formation resistivity. One advantage of this method is that the damping factor and flatness filter can be adjusted to suit different types of data. The programme creates a resistivity cross-section, calculates the apparent resistivities for that cross-section, and compares the calculated apparent resistivities to the measured apparent resistivities. The iteration continues until a combined smoothness constrained objective function is minimized. The depth of investigation cannot be determined by simple calculation and it depends on the acquisition geometry, the conductivity structures and data errors (Oldenburg and Li, 1999).

### **4.3 Interpretation Technique**

Interpreting the resistivity data consists of two steps: a physical interpretation of the measured data, resulting in a physical model, and a geological interpretation of the resulting physical

parameters(Dahlin, 2001). The large-scale data were interpreted with the state-of-the-art interpretation technique called the 2D smoothed damped least squares inversion algorithm.

The results obtained based on 2D inversion of field data and borehole information was interpreted to determine the lithology of the area. In interpreting LUND Imaging data, computer assistance is needed due to the large amount of data collected from the field. In this work, the RES2DINV software which performs smoothness constrained inversion (automatic model interpretation) using finite difference forward modelling and quasi-Newton techniques (Loke and Barker, 1996b) was used for the interpretation of the data.

#### **4.4 Geologic Section from Borehole Data**

Boreholes are necessary and reliable sources of primary data and Electrical Resistivity Imaging (ERI) interpretations provide secondary information. Although borehole data provide a good sample for a six-inch diameter vertical cylindrical volume, it can be a poor representation of the several square metres surrounding the borehole.

Alternatively, electrical resistivity imaging provides block averages of resistivity. Also, borehole data can be a more expensive data acquisition method when compared to an ERI survey. The 2D inversion results of the survey were correlated with a Borehole Log taken within Barnawa area (Table 4.1) obtained from Connate Geosciences and Engineering Limited, Barnawa, Kaduna State. The Log shows an overburden made up of two layers, 10m thick. The first layer is composed of topsoil, 0-2m thick with resistivity ranging between 123 $\Omega$ m to 126 $\Omega$ m. The second layer is made up of laterite about 8m thick with resistivity ranging from 157 $\Omega$ m to 180 $\Omega$ m. The Weathered Basement lies immediately beneath the overburden with thickness of about 15.0m and resistivity value of 147 $\Omega$ m. The rise in

resistivity of 170Ωm to 230Ωm suggests a more compact weathered basement which extends to a depth of about 21.0m. The Fresh Crystalline basement rock is encountered at a depth of 22m with resistivity value greater than 230Ωm and is believed to extend continuously downward from this depth.

**Table 4.1: A Borehole Lithology of “Salient Shopping Mall”, Barnawa (obtained from Connate Geosciences and Engineering Limited, Kaduna,2014).**

Soil and Rock Type	Depth(m)	Resistivity(Ωm)
Top soil	0-2	123-126
Laterite	2-10	157-180
Weathered basement: Gravel, brownish fine to medium grained sand, clay	10-15	147
More Compact weathered basement	15-21	170-230
Fresh crystalline basement rock	22-∞	>230

#### 4.5 Typical Resistivity Values from Previous Works

Resistivity values obtained from previous works (Tables 4.2 and 4.3) in different basement areas of Kaduna State were used to correlate the results of the present survey.

**Table 4.2: Typical Resistivity values compiled from previous works (Baimba, 1978 and Okwueze, 1978).**

Rock type	Resistivity ( $\Omega\text{m}$ )
Clay –fresh water	30-70
Dry clay	40-100
Weathered basement	50-100
Laterite	200-400
Slightly weathered basement	200-500
Dry sand	500-1000
Fresh basement (crystalline)	>1000

**Table 4.3: Typical Resistivity values of rock materials (After Eduvie, 1998; Dan-Hassan and Olurunfemi, 1999; Aboh, 2001; Reynolds, 2003).**

Soil and rock types	Resistivity range ( $\Omega\text{m}$ )
Unconsolidated Wet Clay	20
Clay (very clay)	50-150
Clayey sand soil	30-60
Sandy soil with clay	60-100
Sand and Gravel	30-225
Lateritic soil	120-750
Laterite	800-1500
Unsaturated landfill	30-100
Saturated landfill	15-30
Fresh groundwater	10-100
Weathered biotite granite	50-100
Weathered granite (low biotite)	50-140
Fractured Basement rock	400-900
Granite	100(wet)- $10^6$ (dry)

**Table 4.4: Resistivity values adopted for this work**

<b>Soil and Rock type</b>	<b>Resistivity range (<math>\Omega\text{m}</math>)</b>
Topsoil: Laterite	49 – 180
Saturated soil	4 – 98
Weathered/Fractured Basement	154 – 300

The fresh basement was not reached.

#### 4.6 Field Results

The electrical resistivity images of the earth's subsurface obtained in the study area are presented in Figures 4.1- 4.7. The resistivity models shown were obtained by the optimization technique of RES2DINV by minimizing the difference between the calculated and measured pseudosections of the apparent resistivity data sets. The RMS obtained for the inverse models range from 2.5 - 23.7%. This high range of RMS value is attributable to the small number of data points taken in the sequence of measurement in the field for building the pseudosections. There is a good correlation between the subsurface images depicted by the models. The optimization method basically tries to reduce the difference between the calculated and measured apparent resistivity values by adjusting the resistivity of the model blocks. An initial (starting) model, which is generated automatically by the programme, is then modified to reduce the differences between the model response and the measured data. A measure of this difference is given by the RMS error. This process continues iteratively until the RMS error is reduced to an acceptable limit. However, the model with the lowest possible RMS error is usually chosen, but can sometimes show large and unrealistic variations in the model resistivity values and might not be the best model from a geological perspective. The most prudent approach is to choose the model at the iteration after which the RMS error does not change significantly (Batayneh, 2006). The 2D electrical images along the profiles and their interpretations are discussed in this section. Seven profiles were taken for this survey. Five of them, profiles 2,4,5,6 and 7 were taken in the South-East to North-West direction while profiles 1 and 3 were West-East trending. Forty-two (42) electrodes were used giving a total length of 82.0m and depth reached as 17.2m for six (6) of the profiles (1,2,3,4,5 and 6). Due to inadequate space along profile 7, only thirty-two (32) electrodes were used giving a total length of 64.0m and depth of 12.5m. The inversion result for each profile (Figures 4.1 to 4.7) shows the images of the pseudosections (geoelectric sections)

obtained from the processed data. The results show three distinct images for each profile. The upper image is a plot of the measured (observed) apparent resistivity pseudosection. The middle image is the calculated apparent resistivity pseudosection and the lower image is the true resistivity model obtained after a definite number of iterations of the inversion programme.

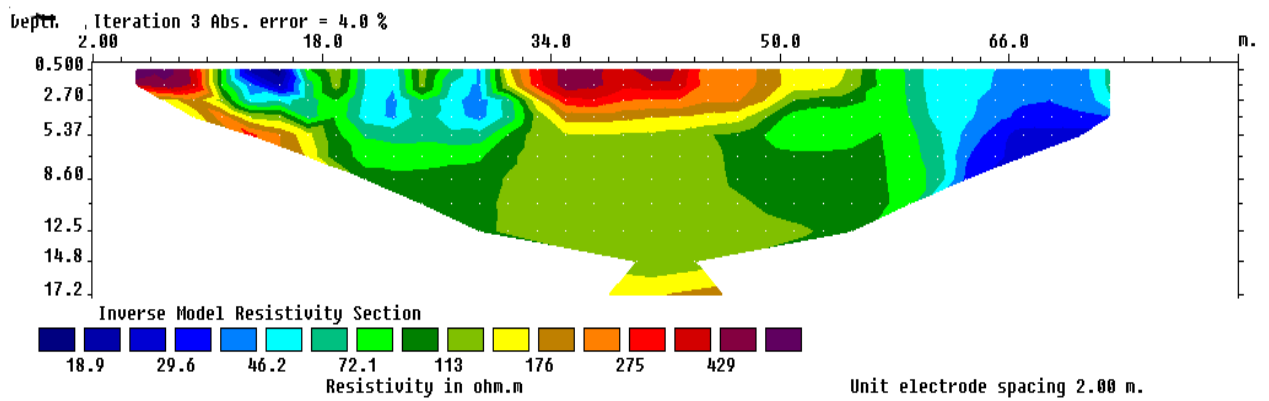
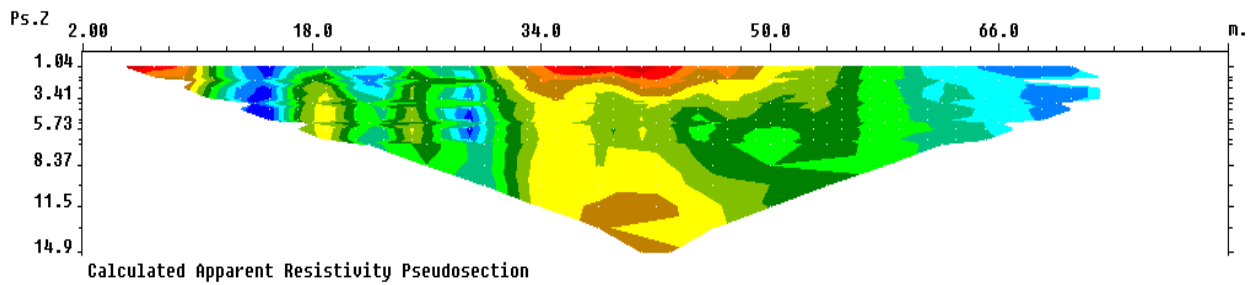
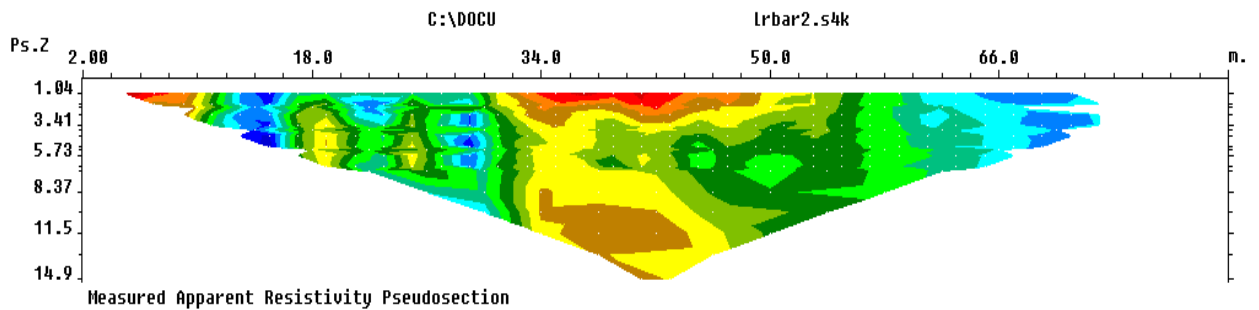
#### **4.6.1 PROFILE 1**

Figure 4.1 shows the measured, calculated apparent resistivity pseudosections and resistivity inversion results for profile 1. Thus, indicating that good fit between the measured and calculated apparent resistivity data was achieved. The inverse resistivity model section shows portions of low resistivity zones along the profile at a distance from 26m to 36m as well as at a distance between 42m and 48m on the surface, with resistivity values ranging from 16Ωm to 30Ωm. This is due to decomposed organic materials and a septic tank existing at the surface. The low resistivity zones are underlain by highly resistive material with resistive value of 154Ωm at a depth of about 5.37m. This low resistivity value indicates a weathered basement hence the fresh basement was not reached. The 2D resistivity values depict an increase in resistivity with depth.

#### **4.6.2 PROFILE 2**

The profile shows patches of low resistivity ranging from 18Ωm to 46Ωm between 12.00m and 14.00m, 21.00m and 23.00m and 28.00m to 30.00m along the profile and to a depth of about 5.37m. These low resistivity zones are as a result of a refuse dump site which is composed of organic materials and an abandoned well which has been filled up with refuse. A high resistivity zone also exists at a depth of about 5m with lateral distance of about 30m to 50m with resistivity range of 275Ωm to 429Ωm. The image profile also shows a low resistivity zone ranging from 18Ωm to 46Ωm at a distance of about 54m to 72m, which is likely to be wet soil. The depth to basement is 17.2m.





**Figure 4.2: Result of 2D inversion of the Schlumberger array data along profile 2**

#### **4.6.3 PROFILE 3**

The resistivity image for profile 3 shows significant, well-defined geological features. The profile shows the top soil composed of highly resistive material ranging from 388 $\Omega$ m to 548 $\Omega$ m at a depth of about 2.7m from the surface. This is likely due to the observed dry and consolidated lateritic clay top soil. Low resistivity values ranging between 49 $\Omega$ m and 98 $\Omega$ m was observed from a depth of 2.7m to about 12.5m from a distance of about 50m to about 74m. This is due to the well present there. The weathered basement ranges between 2.7m and 17.2m. The basement was not reached.

#### **4.6.4 PROFILE 4**

Figure 4.4 shows the measured, calculated resistivity pseudosections and resistivity model of profile 4. The inverse resistivity model shows a highly resistive material of resistivity value ranging from 234Ωm to 982Ωm. The depth range of this material between lateral distances of 12.0m to 22.0m is about 7.5m. This could be attributed to a deeply seated septic tank that is partially filled. It is probably a void. There is a low resistivity zone at a distance of about 40.0m which extends downwards to a depth of about 11.5m. This is reflective of the subsurface owing to the presence of a septic tank and excavated portions which have been filled with refuse/organic materials. The depth to basement is 17.2m.

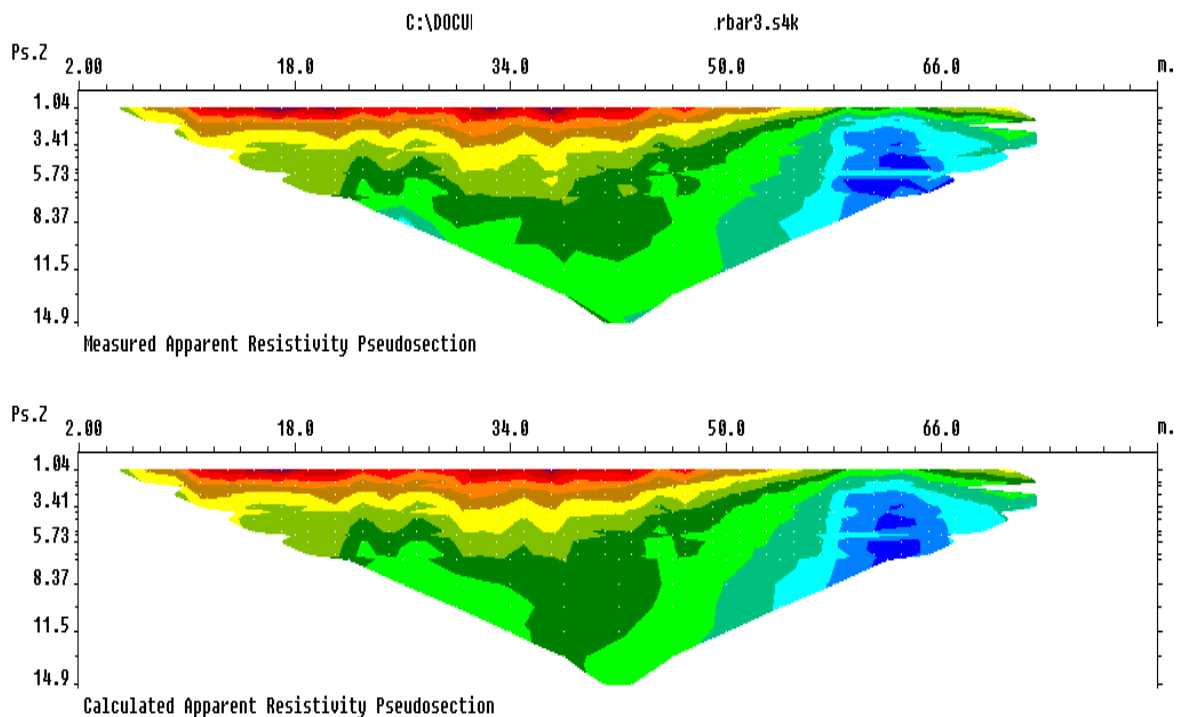
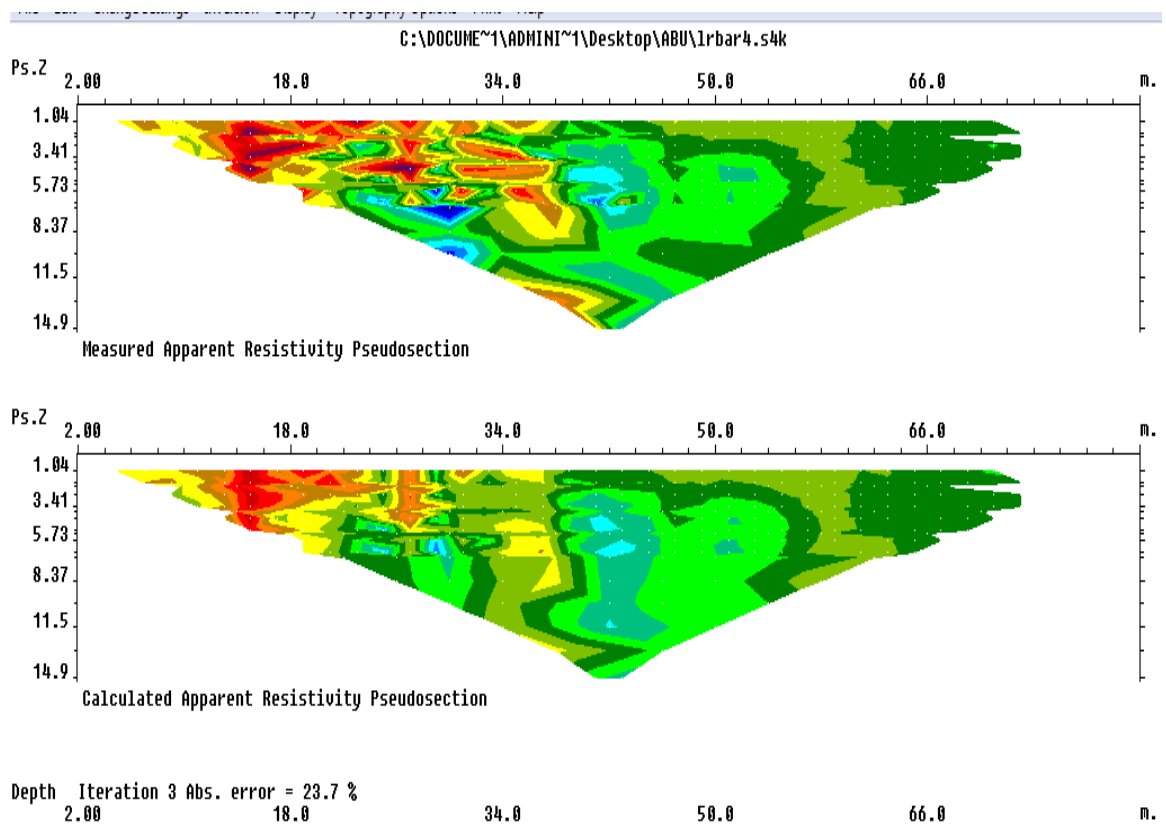


Figure 4.3: Result of 2D inversion of the Schlumberger array data along profile 3



**Figure 4.4: Result of 2D inversion of the Schlumberger array data along profile 4**

#### **4.6.5 PROFILE 5**

The inverse resistivity model shows that the topsoil is of high resistive material with values ranging from  $180\Omega\text{m}$  to  $300\Omega\text{m}$  which could be as observed dry and consolidated lateritic clay top soil at a distance of about 30m to 40m. Between lateral distances of 14m to 20m and 62m to 72m, are low resistivity zones of resistivity values ranging from  $8\Omega\text{m}$  to  $23\Omega\text{m}$ . These portions of low resistivity are of high moisture content (well) and a refuse dump site respectively. The low resistivity value of  $300\Omega\text{m}$  reveals the weathered basement to a depth of about 17.2m hence the basement was not reached.

#### 4.6.6 PROFILE 6

Figure 4.6 shows a low resistivity zone flanked on both sides by high resistive bodies. This occurs at a depth of about 5.37m to 12.50m. This zone with resistivity values ranging from  $10\Omega\text{m}$  to  $22\Omega\text{m}$  is typical of unconsolidated wet clay. At a distance of about 36m to 38m, a possible fracture/ zone of weakness along the profile can be inferred. The depth to basement is about 14.8m.

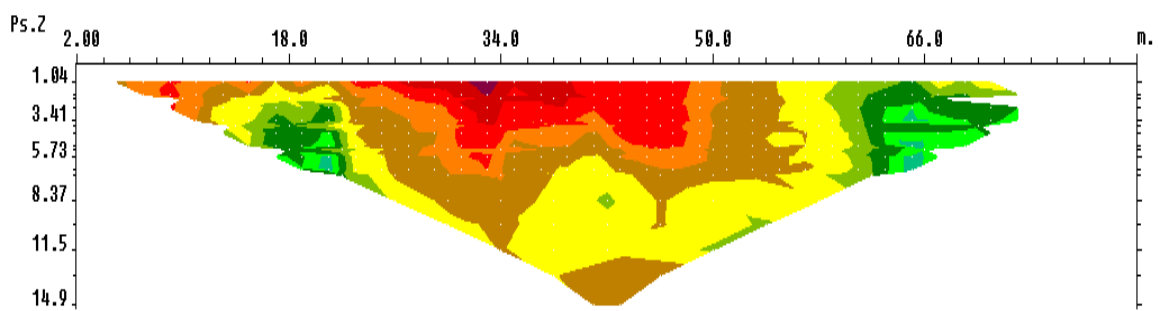
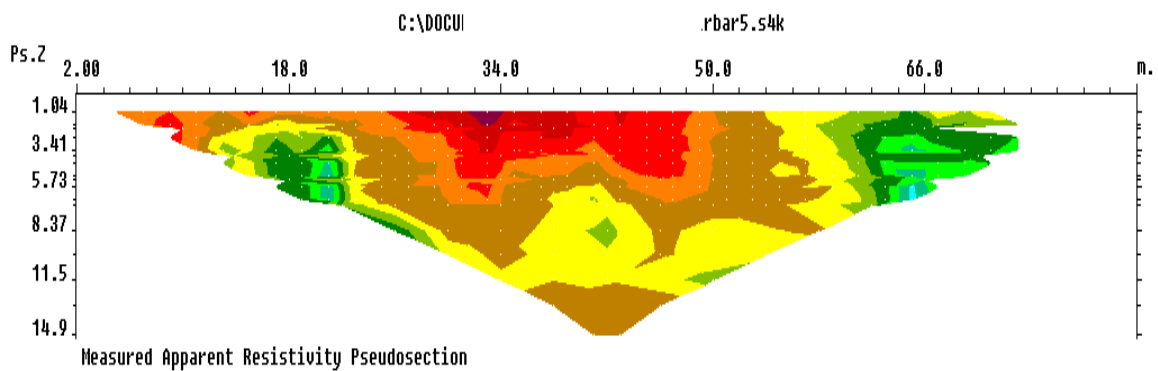
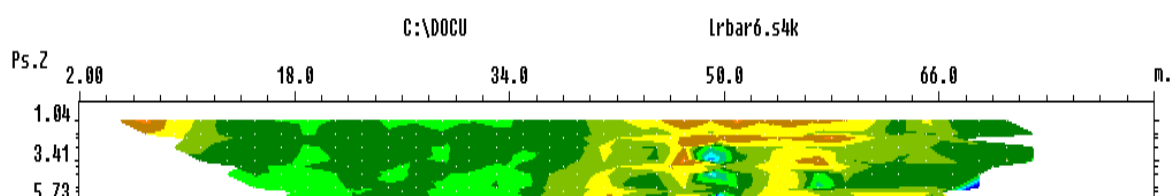


Figure 4.5: Result of 2D inversion of the Schlumberger array data along profile 5





#### **Figure 4.6: Result of 2D inversion of the Schlumberger array data along profile 6**

#### **4.6.7 PROFILE 7**

The resistivity image of profile 7 shows significant, well-defined geological features (Figure 4.7). The profile covers a distance of 64m and depth 12.5m. A total number of 32 electrodes were used. Highly resistive materials with resistivity values ranging from 137 $\Omega$ m to 183 $\Omega$ m were observed at a distance ranging from 0 to 38.0m and depth of 0 to about 8.6m. This is significant due to the observed dry and consolidated lateritic clay top soil. At a distance of about 26.0m to 38.0m reveals that the basement is fractured or partially weathered. At a distance of about 40m, there is a low resistivity zone ranging from a depth of 2.7m to about 8.6m. This is a weak zone. This zone with resistivity ranging from 24 $\Omega$ m to 43 $\Omega$ m is flanked on both sides by highly resistive materials. Weathering probably accounts for the gradual change from moderately high resistivity zone to a lower resistivity zone. It is composed of materials inferred to be decomposed organic materials and vegetable remains as well as seepages from a lavatory section which were evident on the surface. At a distance of about 34.0m to 38.0m from a depth of about 6.91m is the basement in form of an intrusion.

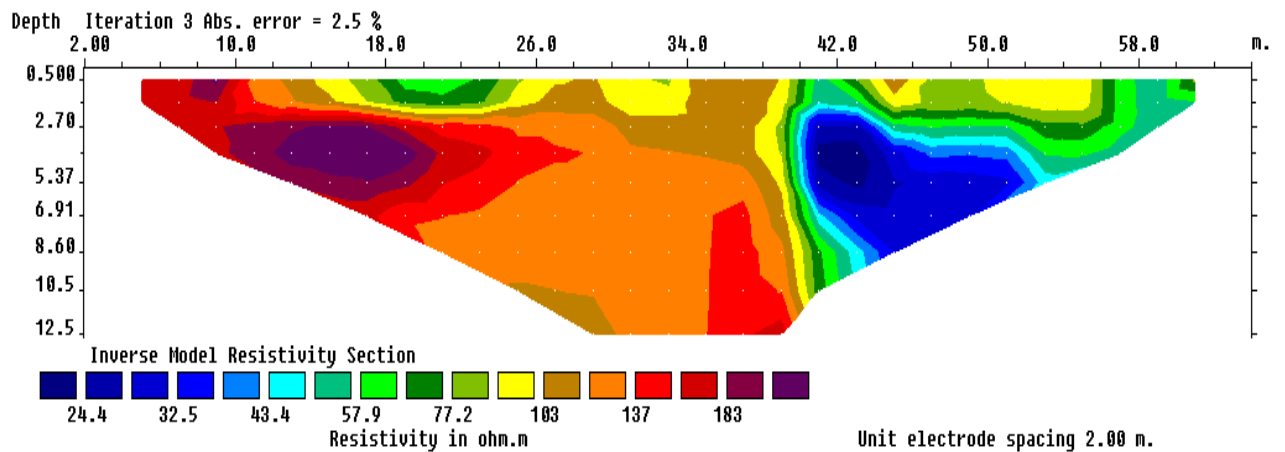
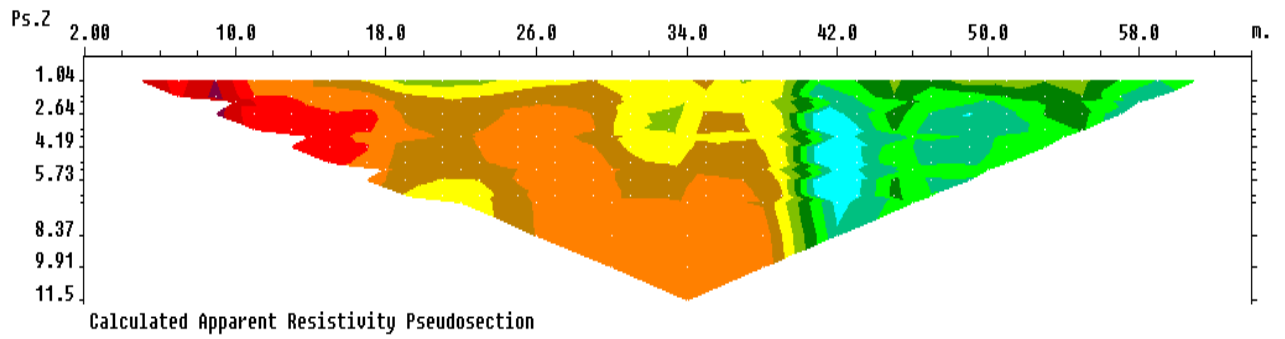
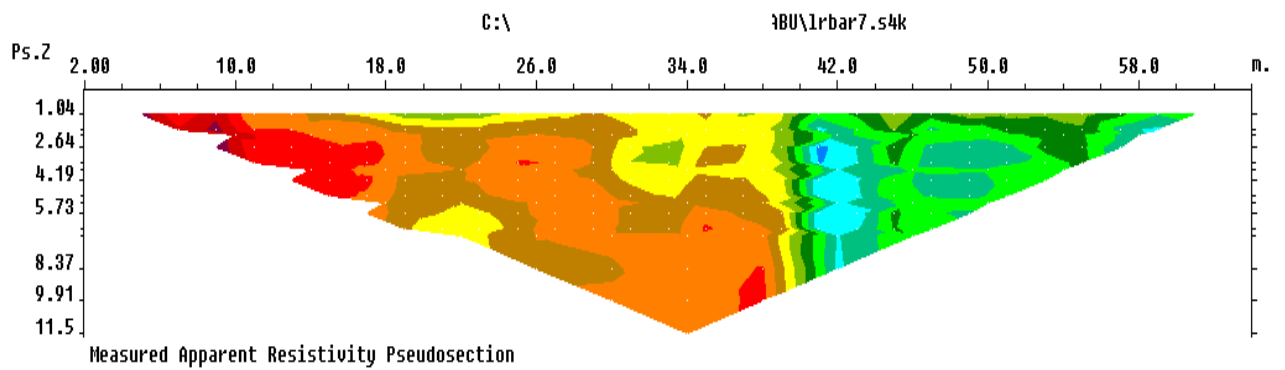


**Figure 4.7: Result of 2D inversion of the Schlumberger array data along profile 7**

Stacked inversion sections of five ERT profiles (Figure 4.8) well depict subsurface lithologies and zones of weakness.

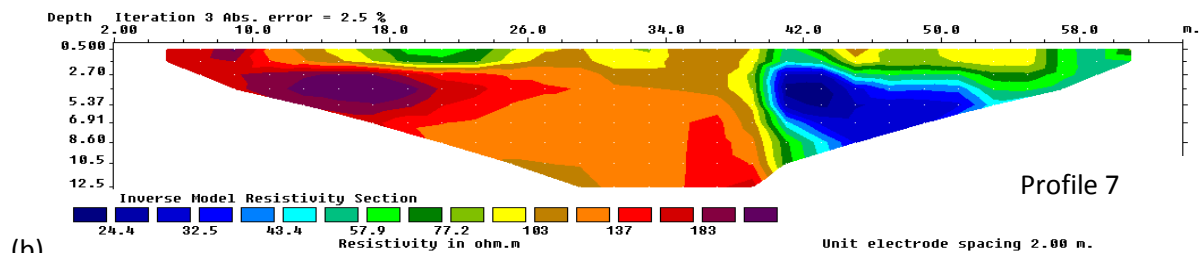
A zone of weakness can be observed across Figure 4.8a (profile 7) at a distance between 38m and 40m with resistivity value between 57 $\Omega$ m and 103 $\Omega$ m to Figure 4.8b (profile 2) at a distance of about 60m with resistivity value ranging from 18 $\Omega$ m to 46 $\Omega$ m. The same observation can be inferred across Figure 4.8c (profile 6) between lateral distance of about 38m with resistivity value ranging from 49 $\Omega$ m to 109 $\Omega$ m to Figure 4.8d (profile 5) at a distance of about 22.0m. This can be a sign of weak zone striking in a direction across these profiles.

Figure 4.8a (profile 7) shows the weathered basement from a depth of about 5.0m to 12.5m with resistivity value ranging from 71 $\Omega$ m to 183 $\Omega$ m and the basement in form of an intrusion at a depth of about 6.91m. The thickness of the weathered basement in Figure 4.8b (profile 2) is between 5.0m and

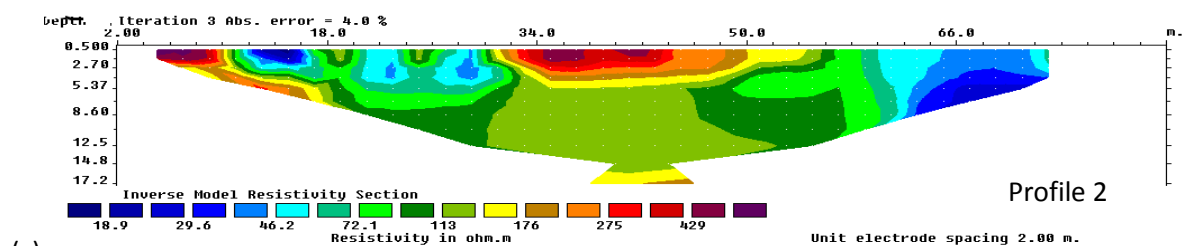
17.1m with resistivity value between 72Ωm and 275Ωm and depth to basement is 17.2m. In Figure 4.8c (profile 6), the thickness of the weathered basement ranges from 0.5m to about 14.8m with resistivity value between 49Ωm and 533Ωm. The depth to basement is 14.8m. Figures 4.8d (profile 5) reveals the presence of the weathered basement rock up to a depth of about 17.2m with resistivity value ranging from 108Ωm to 300Ωm while Figure 4.8e (profile 4) reveals the weathered basement from a depth of about 0.5m to 17.2m with resistivity value ranging from 119Ωm to 460Ωm. The depth to basement is 17.2m.

Figure 4.9a (profile 3) reveals the thickness of the weathered basement ranging from 2.7m to 17.2m thus, the basement was not reached. The resistivity value of the weathered basement is between 138Ωm and 275Ωm. In Figure 4.9b (profile 1), the low resistivity value of 154Ωm indicates the weathered basement. This occurs at a depth of about 5.0m to 17.2Ωm.

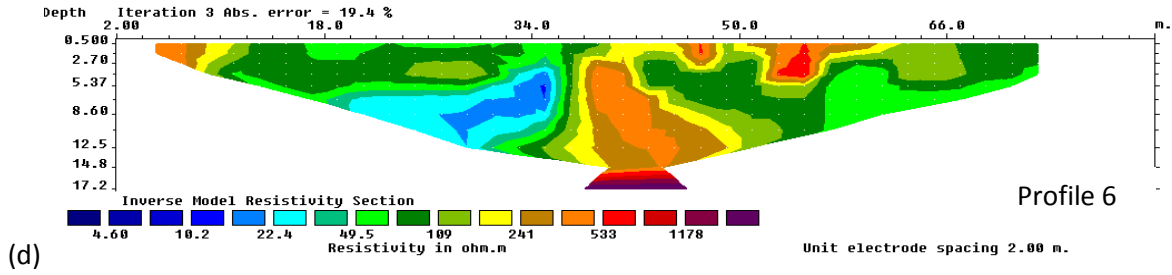
(a)



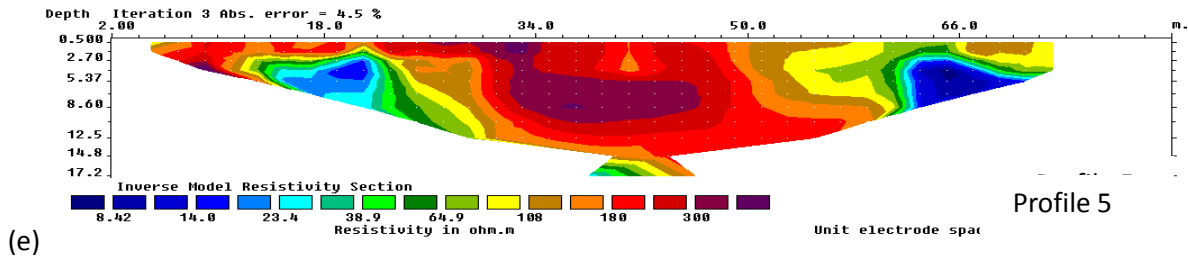
(b)



(c)



(d)



(e)

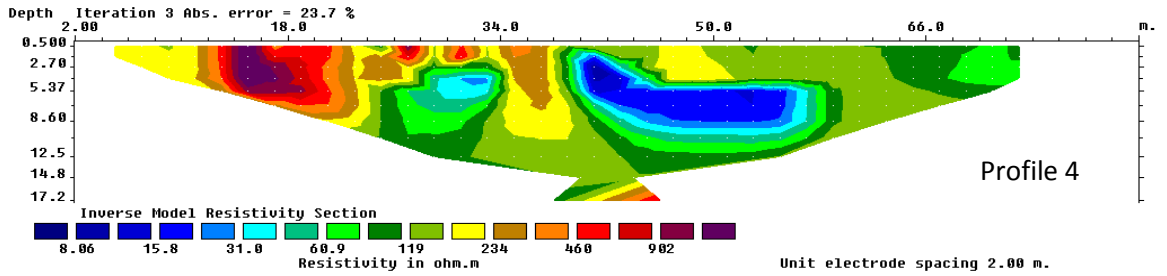
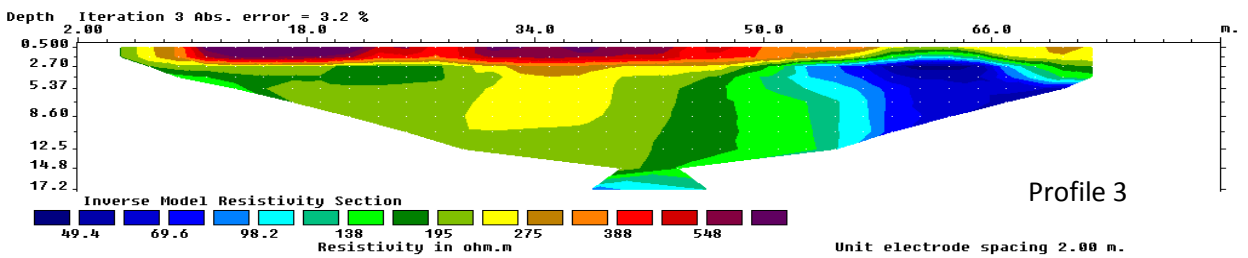


Figure 4.8(a-e):ERT images for profiles 7,2,6,5 and 4 arranged in the order in which they appear within the area of study (see Figure 3.1)

(a)



(b)

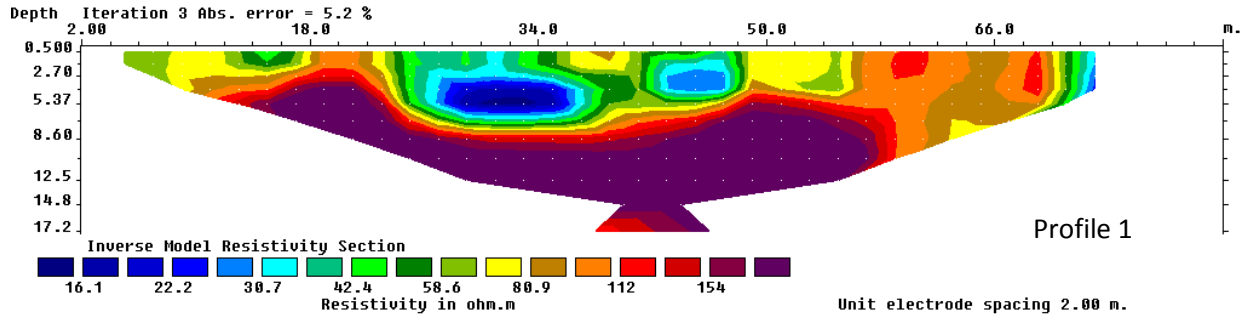


Figure 4.9(a-b):ERT images for profiles 3 and 1 arranged in the order in which they appear within the area of study (see Figure 3.1)

## CHAPTER FIVE

### DISCUSSION, CONCLUSIONS AND RECOMMENDATIONS

#### 5.1 Discussion

The resistivity range lies between 1 to about 1178 $\Omega$ m, indicating variation in soil matrix, grain size distribution and water saturation. The near surface materials, up to a depth of about 2.7m, have moderately high resistivity ranging from 49 $\Omega$ m to 180 $\Omega$ m. The decrease in resistivity at a depth below the top soil indicates the presence of saturated soil with resistivity ranging from 4 $\Omega$ m to 98 $\Omega$ m. This depth varies between 2.7m and 8.6m. The weathered/fractured basement has resistivity values between 49 $\Omega$ m and 533 $\Omega$ m. Its thickness ranges between 5.0m and 17.2m. The fresh basement has variable depth with resistivity value ranging between 429 $\Omega$ m and 1178 $\Omega$ m.

It was observed in Figures 4.8 and 4.9 that the variation in the topography of the basement within the study area is rugged. It is shallow at the northern part (profile 1), middle part (profiles 5 and 6) and eastern parts (profile 4) of the area. These sharp variations can lead to uneven settling of the buildings which can further lead to collapse, and is a probable factor which led to the collapse of the one of the buildings. The zones of weakness that were identified across profiles 7 to 2 and 6 to 5 in Figure 4.8 were also contributing factors responsible for the instability of the buildings.

## 5.2 Conclusions

Electrical imaging has been useful in imaging the subsurface structures within the housing estate located at Barnawa-Narayi junction, Barnawa, Kaduna State. This was with a view to detecting any geological features that may pose danger to the buildings. The 2D electrical resistivity data were acquired using the ABEM Lund multielectrode resistivity meter system. The acquired apparent resistivity data was interpreted using the RES2DINV software. Results of the interpretation showed that the near-surface materials comprise mostly of laterite with resistivity between  $49\Omega\text{m}$  and  $180\Omega\text{m}$  while the underlying materials with high degree of saturation constitute the saturated soil with resistivity ranging from  $4\Omega\text{m}$  to  $98\Omega\text{m}$ . Geologic features suspected to be fractures were identified across profile 7 between lateral distance of 38m and 40m with resistivity value between  $57\Omega\text{m}$  and  $103\Omega\text{m}$  and profile 2 at a distance of about 60m. These features were also identified across profile 6 at a lateral distance of about 38m with resistivity value ranging from  $49\Omega\text{m}$  to  $109\Omega\text{m}$  and profile 5 at a distance of about 22.0m. The models did not suggest the presence of clay that may constitute any problem to the buildings. The depth to basement is variable. This depth in profiles 2 and 4 is 17.2m and in profile 6 it is 14.8m. The basement was not reached in profiles 1, 3, and 5. It appears in form of an intrusion in profile 7 at a depth of about 6.9m. The weathered/fractured basement within the study area has thickness ranging between 5.0m and 17.2m. These are attributed to differential weathering effect of the basement and depositional processes. Based on these results, the basement is shallow towards the north and increases with depth southwards. The 2D resistivity section has confirmed that the depth to competent layer is shallow towards the north and eastern parts of the survey area.

### **5.3 Recommendations**

Based on the result of the research work, the following are recommended:

- a) Seismic technique can be employed in order to compliment the results obtained from the resistivity technique.
- b) Physio-chemical analysis of soils and rocks should be carried out in order to determine the properties and obtain information about soil conditions.
- c) Government should as a matter of national priority discourage the practice of constructing heavy buildings without initially performing geophysical surveys.

## REFERENCES

- Abdullahi, N.K., Udensi, E.E., Iheakanwa, A. and Eletta, B.E. (2014): Geoelectrical Method Applied to Evaluation of Groundwater Potential and Aquifer Protective Capacity of Overburden Units. *British Journal of Applied Science & Technology*, 4(14), 2024-2037.
- ABEM Instrument AB, (2010): Terrameter SAS1000/4000 LUND Imaging System Introduction Manual.
- Aboh, H.O. (2009): Assessment of the Aquifers in Some Selected Villages in Chikun Local Government Area, Kaduna State, Nigeria. *Science World Journal*, Vol. 4 (No 2), P. 37-42.
- Aboh, H.O. (2001): Detailed Regional Geophysical Investigation of the Subsurface Terrain in Kaduna Area, Kaduna State. Unpublished PhD Thesis: Department of Physics, Ahmadu Bello University, Zaria, Nigeria.
- Adukwu, G.O. and Fadele, S.I. (2012): Relevance of Geophysics in Foundation Evaluation in a Typical Basement Complex of North-Western Nigeria. *The Pacific Journal of Science and Technology*, Volume 13, Number 2, P.490-497.
- Alheri, A. and Jatau B. S. (2009): Determination of the Weathered Regolith using Seismic Refraction Method in parts of Kaduna South Industrial Area, Kaduna, Nigeria. *Journal of Engineering and Industrial Applications*, 5(1), P. 74-84.
- Andrews, N.D., Aning, A.A., Danuor, S.K. and Noye, R.M. (2013): Geophysical investigations at the proposed site of the Kwame Nkrumah University of Science and Technology (KNUST) teaching hospital building Kumasi, Ghana, using 2D and 3D resistivity imaging techniques. *International Resource Journal of Geology and Mining*, 3(3), 113-123.
- Baimba, A.B. (1978): Resistivity and Refraction Seismic methods for groundwater Exploration at Zango, Kaduna State. Unpublished M.Sc. Thesis: Department of Physics, Ahmadu Bello University, Zaria, Nigeria.

- Batayneh, A. T. (2006): Resistivity Tomography as an aid to planning gas-pipeline construction, Risha Area, North-East Jordan. *Near Surface Geophysics*, Vol. 4, P.313 – 319.
- Burger, R.H. (1992): 'Exploration Geophysics of the Shallow Subsurface'. Prentice Hall, U.S.A. PP. 30-56.
- Burland, J.B. and Burbidge, M.C. (1981): Settlement of Foundations on Sand and Gravel. *Proceedings of the Institution of Civil Engineers*, 78(1), pp. 1325- 1381.
- Cardarelli, E. and Fischanger, F. (2006): 2D data modelling by Electrical Resistivity Tomography for Complex Subsurface Geology. *Geophysical Prospecting*, Vol.54, P. 121 – 133.
- Chiemeke, C.C. and Osazuwa, I.B. (2007): Application of Seismic Refraction Tomography for Subsurface Imaging in Central Northern Nigeria. *Nigeria Journal of Physics*, 19(2), 247 - 252.
- Connate Geosciences and Engineering Limited, Kaduna. (2014): Report of Geophysical Survey for Groundwater Development at "Salient Shopping Mall", Barnawa, Kaduna.
- Dahlin, T. (2001): The Development of Electrical Imaging Techniques. *Computers and Geosciences*, 27(9), 1019-1029.
- Dan-Hassan, M.A. and Olurunfemi, M.O. (1999): Hydrogeophysical investigation of a Basement Terrain in the North-Central part of Kaduna State, Nigeria. *Journal of Mining and Geology*, 35 (2), 189-206.
- Eduvie, M.O. (1998): Exploration, Evaluation and Development of groundwater in Southern part of Kaduna State, Nigeria. PhD Thesis, Department of Geology, Ahmadu Bello University, Zaria, Nigeria.
- Egwuonwu G. N., Ibe, S.O. and Osazuwa, I. B. (2011): Geophysical Assessment of Foundation Depths around a Leaning Superstructure in Zaria Area, Northwestern Nigeria using Electrical Resistivity Tomography. *The Pacific Journal of Science and Technology*, 12(1), 472-486.

- Fadele S.I, Jatau B.S. and Umbugadu A. (2012): Engineering Geophysical Investigation around Ungwan Doka, Shika Area within the Basement Complex of North-Western Nigeria. *Journal of Environment and Earth Science*, Vol. 2, No.7, P.17-28.
- Giano S.I., Lapenna, V., Piscifelli, S. and Schiattarella, M. (2000): Electrical imaging and self potential surveys to study geological setting of the quaternary slope deposits in the agri-high valley. *Annali de Geofisica*, 43, 409-419.
- Grant, F.S. and West, G.F. (1965): Interpretation theory in Applied Geophysics. McGraw Hill Book Company, New York.
- Griffiths, D. H. and Barker, R. D. (1993): Two-dimensional resistivity imaging and modelling in areas of complex geology. *Journal of Applied Geophysics*, 29, 211-226.
- Jatau, B. S., Fadele, S. I. and Agelaga, A. G. (2013): Groundwater Investigation in Parts of Kaduna South and Environs using Wenner Offset Method of Electrical Resistivity Sounding. *Journal of Earth Sciences and Geotechnical Engineering*, Vol. 3, No. 1, 41-54.
- Loke, M.H. (2000): Electrical Imaging Surveys for Environmental and Engineering Studies: A Practical Guide to 2D and 3D Surveys. [www.terraip.co.jp/lokenote](http://www.terraip.co.jp/lokenote). P. 59.
- Loke, M. H. (2004): Tutorial : 2-D and 3-D Electrical Imaging Surveys. (From the internet, Pp 1- 136).
- Loke, M.H. and Barker, R.D. (1996a): Practical Techniques for 3D Resistivity Surveys and Data Inversion. *Geophysical Prospecting*, 44, 499-523.
- Loke, M.H. and Barker, R.D. (1996b): Rapid Least-Squares Inversion of Apparent Resistivity Pseudosections by a Quasi-Newton Method. *Geophysical Prospecting*, Vol.44, P.131-152.

- McCury, P. (1976): The Geology of the Precambrian to Lower Paleozoic rocks of Northwestern Nigeria. A review in Kogbe, C.A. (Ed), Geology of Nigeria. Elizabethan Publishing Company, Lagos, P. 15-39.
- Obaje, N.G., (2009): Geology and Mineral Resources of Nigeria. Springer, Berlin, Germany, ISBN-13: 9783540926849. P. 221.
- Okwueze, E. E. (1978): Geophysical exploration for groundwater in Kankarg KadunaState; Unpublished M.Sc. Thesis, Department of Physics, Ahmadu Bello University, Zaria, Nigeria.
- Olabode, T.O., Olaniyan, I.O., and Onugha, A. (1999): Optimum drilling depth in the Crystalline Basement of Nigeria. Kaduna Polytechnic, College of Engineering Conference series, Vol.20, P. 10-18.
- Oldenburg, D.W. and Li, Y. (1999): Estimating depth of investigation in D.C. Resistivity and IP surveys. Geophysics, Vol. 64 (2), P. 403-416.
- Oyedele, K.F. (2011): Application of Geophysical and Geotechnical Methods to Site Characterisation for Construction Purposes at Ikoyi, Lagos, Nigeria. *Journal of Earth Science and Geotechnical Engineering*, Vol.1, No.1, P. 87-100.
- Preeze, J. W. and Barber, W. (1965): Distribution and chemical quality of groundwater in Northern Nigeria. Geological Survey of Nigeria Bulletin No 36, PP 60-63.
- Reynolds, J.M. (2003): An Introduction to Applied and Environmental Geophysics. John Wiley and Sons, Reynolds Geosciences Ltd., UK.
- Russ, W. (1957): The Geology of parts of Nigeria, Zaria and Sokoto Provinces. Published by the Authority of Federal Government of Nigeria.

- Sands, T.B. (2002): Buildings Stability and Tree Growth for in Swelling London Clay- Implications for Pile Foundation Design. [www.agu.org](http://www.agu.org) .
- Telford, W. M., Geldart L.P. and Sheriff R.E. (1990): Applied Geophysics. Cambridge University Press, London.
- Tomlinsong, M.J. and Boorman, R. (1999):*Foundation Design and Construction*. Longman Scientific and Technical: Singapore. 1- 125.
- Ugwu, G. Z. (2012): Electrical resistivity imaging for the investigation of the subsurface formations at Bethel Estate in Emene Industrial Layout, Enugu, Southeastern Nigeria. *ASUU-ESUT Jour. Sci. Tech. Human.*, 1(1), 112-119.
- Ugwu, G. Z. and Ezema P. O. (2013): 2D Electrical Resistivity Imaging for the Investigation of the Subsurface Structures at the Proposed Site for Kauridan Estate at Ibagwa – Nike, Southeastern Nigeria.*International Journal of Scientific Research in Knowledge (IJSRK)*, 1(12),P. 528-535.